A Scheme to Account for the Effects of Rb^+ and K^+ on Inward Rectifier K Channels of Bovine Artery Endothelial Cells

PETER S. PENNEFATHER* and THOMAS E. DECOURSEY‡

From the *Faculty of Pharmacy, University of Toronto, Toronto, Ontario, M5S 2S2, Canada; and ‡Department of Physiology, Rush Presbyterian St. Lukes Medical Center, Chicago, Illinois 60612

ABSTRACT An electrochemical gating model is presented to account for the effects described in the companion paper by M. R. Silver, M. S. Shapiro, and T. E. DeCoursey (1994. *Journal of General Physiology.* 103:519–548) of Rb^+ and Rb^+/K^+ mixtures on the kinetics and voltage dependence of an inwardly rectifying (IR) K^+ channel. The model proposes that both Rb^+ and K^+ act as allosteric modulators of an intrinsically voltage dependent isomerization between open and closed states. Occupancy of binding sites on the outside of the channel promotes channel opening and stabilizes the open state. Rb^+ binds to separate sites within the pore and plugs IR channels. Occupancy of the pore by Rb^+ can modify the rates of isomerization and the affinity of the allosteric sites for activator ions. The model also incorporates the proposed triple-barreled nature of the IR channel (Matsuda, H., 1988. Journal of Physiology. 397:237–258.) by proposing that plugging of the channel is a cooperative process involving a single site in each of the three bores, 80% of the way through the membrane field. Interaction between bores during plugging and permeation is consistent with correlated flux models of the properties of the IR channel. Parallel bores multiply the number allosteric sites associated with the macromolecular channel and allow for steep voltage dependence without compromising the parallel shift of the half-activation potential with reversal potential. Our model proposes at least six and possibly 12 such allosteric binding sites for activator ions. We derive algebraic relations that permit derivation of parameters that define simple versions of our model from the data of Silver et al. (1994). Numerical simulations based on those parameters closely reproduce that data. The model reproduces the RS^+ induced slowing of IR kinetics and the negative shift of the relation between the half-activation voltage ($V_{1/2}$) and reversal potential when channel plugging is associated with (*a*) a slowing of the isomerization rates; (*b*) an increase in the affinity of allosteric sites on closed channels that promote opening; and (*c*) a decrease in the affinity of sites on open channels that slow closing. Rb^+ also slows closing at positive potentials where open channel blockade is unlikely.

Address correspondence to Dr Peter Pennefather, Faculty of Pharmacy, University of Toronto, 19 Russell Street, Toronto, Ontario M5S 2S2, Canada.

J. GEN. PHYSIOL. © The Rockefeller University Press · 0022-1295/94/04/0549/33 $2.00
Volume 103 April 1994 549–581

Allowing Rb^+ to be 1.5 times more potent than K^+ as an activator in the model can account for this effect and improves the match between the predicted and observed relation between the Rb^+ to K^+ mole fraction and the opening rate at $V_{1/2}$. Because Rb^+ has a lower permeability then K^+, cation binding sites that regulate gating probably are different from those governing permeation.

INTRODUCTION

In the accompanying paper, Silver, Shapiro, and DeCoursey (1994) have shown that rubidium (Rb^+) can substitute for potassium (K^+) in activating an inwardly rectifying K current, IR, found in endothelial cells obtained from bovine pulmonary artery. However, in the presence of Rb^+, the kinetics and voltage dependence of that gating is modified. If the proportion of the extracellular gating ion that is Rb^+ (e.g., the Rb^+ mole fraction = $[Rb^+]/([Rb^+] + [K^+]) = F$) is increased, there is a negative shift in the reversal potential due to the lesser permeability of Rb^+ and a reduction in conductance resulting from a channel-plugging action of Rb^+. When 160 mM K^+ in the external solution is completely replaced by 160 mM Rb^+, the reversal potential is shifted by −24 mV indicating a Rb^+ permeability 45% that of K^+, and the single channel conductance is reduced to ~3%. The channel-plugging effect is half-maximal around 0 mV in an external solution containing 20 mM Rb^+, 140 mM K^+. In addition to these easily explained actions, as F increases there is an −8 mV shift of the half-activation potential ($V_{1/2}$) of the voltage-activation curve, a reduction in the steepness of that curve, and a slowing of the gating kinetics of the current at voltages around $V_{1/2}$. Here we explore the hypothesis that these additional differences between the behaviour of IR channels activated by Rb^+ and K^+ are primarily a consequence the channel-plugging action of Rb^+.

The open probability and kinetics of opening and closing of IR channels appear to be a function of the binding of K^+ ions to multiple sites on the channel, accessible from the extracellular side of both open and closed states of that channel (Cohen, DiFrancesco, Mulrine, and Pennefather, 1989; Pennefather, Oliva, and Mulrine, 1992); channels responsible for IR-like currents behave like K^+-activated K^+ channels. Activation by K^+ arises because occupancy of binding sites for external activator ions by K^+ on open channels stabilizes that open state while binding of K^+ to similar sites on closed channels promotes isomerization to the open state (Pennefather et al., 1992). The data of Silver et al. (1994) place additional constraints on models of IR channel gating by demonstrating that Rb^+ can replace K^+ at those activator sites in controlling IR gating. In this paper, we examine those constraints and also the possibility that some of the observed changes in the voltage- and time-dependence of IR channel gating produced by replacing external K^+ with Rb^+ can be explained if there is an interaction between occupancy of the channel pore by Rb^+ or K^+ and occupancy of the binding sites for those ions that allosterically regulate channel gating. Because the plugging action occurs at sites distinct from those that modulate gating, differences in affinity of the two classes of sites could give rise to the differences in gating observed as K^+ is replaced by Rb^+. There need not be any differences between external K^+ and Rb^+ in terms of their ability to bind to activator sites and modulate gating. The differences in gating could arise primarily from differences in the ability of K^+ and Rb^+ to plug the channel and thereby create a new

class of states of the channel with modified gating properties. Two key predictions of this model are verified. First, in the absence of external K^+, the voltage-activation curve for IR channels is shown to shift in parallel with ln([Rb^+]). Second, the effects of Rb^+ on gating at potentials around $V_{1/2}$ are related to the fraction of channels that are plugged at those potentials.

Several authors have suggested that IR channels behave as if they are made up of three equivalent and interacting bores that can open and close in a concerted fashion. The main evidence for this is that blocking ions such as intracellular Mg^{2+}, can induce equally spaced subconducting states whose probability exhibits a binomial distribution dependent on the concentration of the blocking ion. Plugged channels appear to be trapped in the open state; such trapping results in bursts of subconductance states with true closure apparently only occurring from the fully open state (Matsuda, 1988; Ishihara, Matsuiye, Noma, and Takano, 1989; Oliva, Cohen, and Pennefather, 1990). At certain potentials, this blockade will lead to a paradoxical increase in the average outward IR current (Ishihara et al., 1989; Oliva et al., 1990). Matsuda, Matsuura, and Noma (1989) reported that concentrations of extracellular Rb^+ and Cs^+ that reduced the open state probability also caused subconductance states but in only 20% of channels; with most channels that were examined, sublevels induced by Cs^+ and Rb^+ in the inward current were not observed. Those ions simply decreased the mean open time of the channels in a concentration dependent manner (Fig. 7, Matsuda et al., 1989). To explain this latter behavior, they suggested that blockade of a single bore could somehow destabilize the other two bores and induce conversion to a closed state. Here we build on that suggestion and explore the possible consequences of channel plugging on channel gating.

To simplify consideration of the plugging of a multi-barrelled channel, we assume that once one bore is plugged by one Rb^+ ion the affinity of the other bores for the plugging ion is greatly increased so that all bores become plugged in a concerted cooperative manner. We assume also that the converse is true, namely, that all three Rb^+ ions must leave for the channel to become unplugged. We also postulate that unlike channels plugged by Mg^{2+}, those channels plugged by Rb^+ can close. Open channels that have been plugged but which have not closed (open-plugged) can be revealed by stepping the membrane potential to positive levels where plugging is reversed more rapidly than channels can close, plugged channels that have closed (closed-plugged) trap the plugging ion in the channel and behave like closed channels, making no contribution to the "instantaneous" current associated with the step to positive potentials. The existence of plugged-closed channels is essential for channel plugging to lead to the observed negative shift in the position of the voltage-activation curve (see Silver et al., 1994). If those plugged channels could not close, channel plugging would always stabilize the open state and shift the $V_{1/2}$ of the voltage-activation curve to positive potentials. The voltage dependence of blockade implies that only open channels can become plugged (see Woodhull, 1973; Neher and Steinbach, 1978; Pennefather and Quastel, 1980).

In this paper we explore the predictions of our model in two ways. First, algebraic solutions to simplified versions of the model are derived and measurable relationships are deduced between independent variables such as membrane potential or the concentration of activating ions and dependent variables such as fractional activation

or time constants of current relaxations following voltage jumps. Second, using parameters derived from the algebraic relations, the model is solved numerically and the predicted kinetic and steady state behavior of the model is compared to experimental data.

GLOSSARY

$'_{U,P}$	Primes indicate experimentally determined approximation of that parameter. Subscripts U and P indicate parameters determined for conditions where channels are mostly unplugged or plugged respectively
IR	Inwardly rectifying K^+ current or channel
A	Effective concentration of activator ions that control the gating of IR channels
G	Effective concentration of permeating ions that carry current through IR channels
P	Effective concentration of ions that plug IR channels
F	Rb^+ mole fraction = $[Rb^+]/([Rb^+] + [K^+])$
m,n	Parameters indicating critical numbers of activator ions involved in various gating processes; m is the number of activator ions required to be bound to unplugged channels before the channel opens; n is the number of gating sites that must be free for the channel to close
m'_U, m'_P n'_U, n'_P	Approximation of m and n, distorted by saturation of binding sites that allosterically modulate gating; subscripts P and U indicate that the parameter was derived data obtained under conditions where the channel was mostly plugged or unplugged respectively
r	total number of binding sites for activator ion; $r = m + n$
C', C_{TP}, C_{TU}, O', O_{TP}, O_{TU}	Closed (C) and open (O) states of the IR channel. The subscripts TU and TP indicate a summation of all unplugged or plugged forms of the states respectively. The prime indicates all forms of the states are considered
$C_U A_m, O_P A_m$	Closed and open substates of the IR channel associated with various numbers of activator ions, A (indicated by the subscripts to A)
L, T	Equilibrium dissociation constants defining the binding of activator ions A to the closed and open states of the channel respectively. When voltage dependence of L and T is considered, the subscript 0 refers to the value of the parameter at 0 mV.
T'	$T' = T/(T + A)$
α, β	Microscopic isomerization rate constants defining rates of opening and closing respectively of closed and open states with the same level of occupancy of gating sites; Subscripts U and P indicate that rates are for interconversion between unplugged and plugged states, respectively
α', β'	Macroscopic opening and closing rates respectively, determined from whole-cell voltage-clamp experiments. Subscript ½ refers to rates recorded at the half-activation potential
E_K, E_{Rb}, E_A	Reversal potential of IR channel with external permeating ion indicated by subscript and internal ion being K^+
$V_{1/2}, V_{U1/2}, V_{P1/2}$	Half-activation potentials subscripts U and P indicate values measured when channels are respectively mostly unplugged due to a low concentration of P or plugged due to a high concentration of P
B	$F/RT = e/kT$ = 25.7 mV at 25°C

x_U, x_P Effective gating charge governing isomerization to the open state from the closed state with Rb^+ mole-fractions of 0 and 1, respectively

y_U, y_P Effective gating charge governing isomerization to the closed state from the open state with Rb^+ mole-fractions of 0 and 1, respectively

k_1 Rate constant for entry of plugging ion into the channel from the outside of the cell

k_{-1} Rate constant for escape of the plugging ions from the channel to the outside of the cell

k_2 Rate constant for escape of the plugging ion from the channel to the cytoplasmic side of the cell

k_- Rate of unplugging of the channel; $k_- = k_{-1} + k_2$

k_+ Rate of plugging of the channel; $k_+ = k_1 P$

z Effective gating charge governing the binding of activator ions A to gating sites

z' Effective gating charge governing voltage dependence of k_{-1}

δ Fraction of the membrane field experienced by the external plugging ion when it binds within the channel and plugs it; $z' = 3\delta$

z'' Effective gating charge governing voltage dependence of k_2

γ Fraction of the membrane field experienced by the plugging ion when it escapes from the blocking site within the channel to the inside of the cell; $z'' = 3\gamma$

P_{Rb}/P_K Ratio of permeabilities to Rb^+ and K^+ of the IR channel

THEORY

Kinetic Scheme

We have developed a modified allosteric model of IR channels that can account for the effects on channel gating associated with changes in the mole-fraction of Rb^+ and K^+. Before discussing our specific model it is instructive to consider a general form of an allosteric model of gating (see Hill and Chen, 1971) and its applicability to the gating of IR channels. We are proposing that each IR channel has r binding sites for activator ions (A) and that each channel can exist in at least four major states: resting and unplugged (C_U), open and unplugged (O_U), open-plugged (O_P) and closed-plugged (C_P). In its general form, the model must consider $4(1 + r)$ substates and $4(1 + r!/(r - 2)!)$ substates if two species of activator ions are involved. For simplicity, to reduce the number of substates that need to be considered, we will assume initially that occupancy of the ion binding sites by either K^+ and Rb^+ has the same effect on a given substate so that the effective concentration of activator ions will remain constant as the mole fraction of Rb^+ changes. Below we show that this assumption needs to be modified slightly for the model to fit the data but it nevertheless is useful in developing the model.

Our aim here simply is to present a type of scheme that could form the basis of an optimized model of IR channel gating. A broader range of experimental data would be required before realistic optimization of parameters could be attempted. Accordingly, we make a large number of simplifying assumptions in order to facilitate the conceptualization, description and simulation of the model and to allow us to illustrate major implications of the model using simple algebraic relations. We

assume that for any one of the four states, all allosteric binding sites that modulate gating are equivalent and equilibrate with A on a time scale that is fast relative to the rates governing isomerization between open and closed forms of the channel. Therefore, the various levels of occupancy of the binding sites can be defined in terms of equilibrium dissociation constants L_U, T_U, T_P and L_P. Because the binding sites are assumed to be equivalent, the effective dissociation constant for a given level of occupancy will simply be the dissociation constant for a single site multiplied by a factor that reflects the multiple ways in which that level of occupancy could develop from or decay to adjacent levels of occupancy. The equivalency assumption reduces the number of parameters that need to be considered to describe a system of the type we are proposing. It is used here merely as a convenience as it facilitates algebraic descriptions of the model.

The rates of channel plugging and unplugging by blocking ions (P) also are assumed to be fast relative to the isomerization rates governing transitions between open and closed states. Thus, a single process, isomerization between open and closed states will dominate the kinetics of the system. To preserve microscopic reversibility and the equivalency of binding sites, any difference between adjacent substates in the affinity of allosteric sites for the same activator ion must be associated with differences in the rates of interconversion between adjacent states that increment as the degree of occupancy of activator sites increases (e.g., for every cyclic pathway within a kinetic scheme, in the steady state, the products of the rates defining a loop of the cycle in one direction must equal the product of rates defining that loop in the opposite direction). These principles are illustrated in Scheme I. In that scheme, the subscripts U and P refer to isomerizations of unplugged and plugged channels respectively.

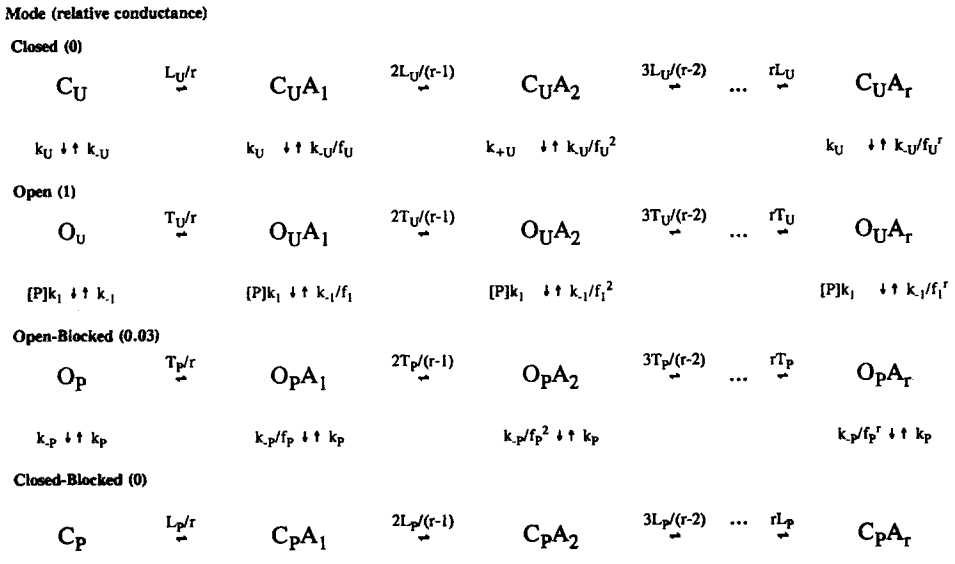

Note: $f_U = (T_U/L_U)$; $f_P = (T_P/L_P)$; $f_I = (T_P/T_U)$

SCHEME I

Pennefather et al. (1992) showed how the kinetic analysis of allosteric models such as Scheme I could be simplified further if it is assumed that isomerizations between open and closed states occur preferentially at one particular level of occupancy so that a single pair of rates dominate microscopic or intrinsic isomerization. Because the binding of gating ions is assumed to be rapid relative to the intrinsic isomerization rates (α and β) and the proportion of open or closed channels in the substate that can isomerize is small, the rate constants α and β will be larger than the macroscopic or effective isomerization rate constants α' and β'. Provided the forward and reverse rates of isomerization between open and closed states are both increased to the same extent at that one level of occupancy, the steady state predictions of such models are the same as the more general allosteric models. Further simplification is obtained by proposing that closed substates with a level of occupancy higher than the isomerizing substate and open substates with a lesser level of occupancy do not exist. Hence, in the specific models considered here we postulate that isomerization occurs preferentially when n of the gating sites are free and m are bound with activating ions. Two versions of the general allosteric model modified in this way (Scheme II *A* and *B*) are presented to illustrate that a range of values of m and n are consistent with our data.

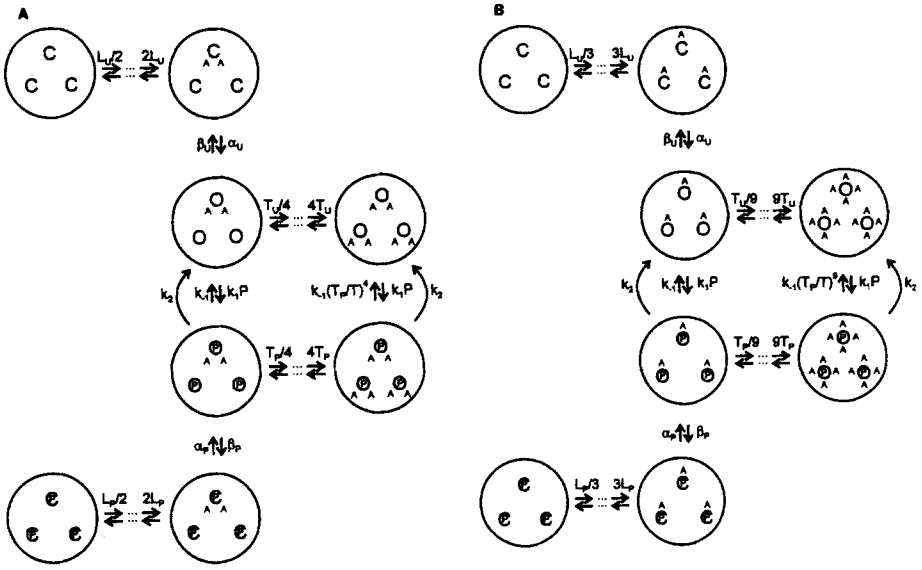

SCHEMES II*A* AND II*B*

Because of evidence that IR channels in cardiac myocytes may consist of three identical pores which usually gate simultaneously (Matsuda, 1988) we have chosen values of m, n, and r that reflect this possible tripartite nature. Another more significant constraint is that m and n must be large enough to account for the steep slope of the line that describes the log–log relation between concentration of activator ion and the activation or deactivation rates. The possible triple-barrelled structure, with each barrel made up of four or more channel subunits (see Kubo,

Baldwin, Jan, and Jan, 1993) would allow large numbers of equivalent binding sites to exist on a single macromolecular structure. In Scheme II *A* we set $m = 2$, $n = 4$, and $r = 6$. In that particular scheme, the sites on the closed channel involved in promoting opening are assigned to a specific bore in order to maintain the equivalency of those sites. In Scheme II *B* we set $m = 3$, $n = 9$, and $r = 12$, the equivalency assumption is maintained by assuming that each closed bore must become associated with one activator ion before channel opening can occur. Although these assumptions have mechanistic and structural implications, at this stage in our understanding of IR channels the assumptions are merely a convenient way of maintaining the equivalency assumption. For simplicity we have assumed that all of the voltage dependence of gating arises from voltage-dependent isomerization between states, this avoids saturation of the voltage dependence of gating kinetics due to saturation of binding sites at large negative potentials relative to $V_{1/2}$ (see Pennefather et al., 1992).

Once the channel is open we propose that it can become blocked or plugged by Rb^+ (see Hagiwara and Takahashi, 1974; Standen and Stanfield, 1980). This process will be governed by a forward rate (k_+) proportional to the effective concentration of blocking ions ($k_+ = k_1[P]$) and a reverse rate (k_-) dependent on two pathways: the first, governed by a rate k_{-1}, reflecting escape of the blocking ion from the channel to the outside of the cell and the second, governed by a rate k_2, reflecting permeation of the blocking ion through the channel to the inside of the cell (hence, $k_- = k_{-1} + k_2$). The model considers the consequences of allowing the affinity of the open state for activator ions to be different if the open state is plugged or not (i.e., T_P and T_U can be different). To preserve microscopic reversibility we multiply k_{-1} by a factor equal to $(T_P/T_U)^n$ where n reflects the number of activator sites that are occupied in the pair of substates being considered (see Scheme I). In both versions of Scheme II we postulate that blockade of any one of the bores by Rb^+ makes it much easier for the other two bores to become blocked. This is slightly different from the model proposed by Matsuda et al. (1989) where blockade of any one barrel caused the other barrels to shut regardless of whether they were plugged. The model also assumes that recovery or unplugging requires that all three Rb^+ molecules leave the triply blocked state of the channel. This simplifies the description of the plugging reaction without ignoring the possibility of multiple bores of the channel and allows this form of blockade to be steeply voltage dependent (i.e., three times greater than if only one Rb^+ ion were involved [see below]). Finally, the model assumes that plugged channels can still isomerize between open and closed configurations, albeit at a rate different from unplugged channels. As with unplugged channels, the gating sites associated with the plugged bores will change their affinity for activator ions upon closure, in this case from T_P to L_P.

It is unlikely that Schemes like II *A* and II *B* are the only ones capable of accounting for our data but they have the advantage of being completely defined by a relatively small number of parameters that can be deduced from our data and therefore make possible mechanistic and explicit interpretations of the effects of Rb^+. The two schemes are considered here simply to illustrate how changes in gating produced by replacing K^+ by Rb^+ could arise provided that Rb^+, in addition to activating the channel also plugged it in a manner that influenced the affinity of activator ions. The implications of these schemes for the relation between various

factors such as membrane potential or concentration of K^+ or Rb^+ and the steady state level and time-dependence of IR channel activation and blockade are explored in the Appendix with a view of estimating from the experimental data the parameters that define schemes of these types. In the next few sections we summarize and discuss those considerations.

Time and Concentration Dependence

It is apparent that with both Scheme II *A* and *B* that the macroscopic rate of opening α' will be dependent on the intrinsic or microscopic closed to open isomerization rates (α_U, α_P) and the proportion of channels that are in the closed substates that isomerize preferentially (e.g., $C_U A_m$ and $C_P A_m$). The rate of closing will be defined similarly. In the Appendix (Eq. A4) we show that when the concentration of Rb^+ is low and presumably $k_+ \ll k_-$ (but see below),

$$\alpha'_U = \alpha_U \left(\frac{K}{L_U + K}\right)^m; \beta'_U = \beta_U \left(\frac{T_U}{T_U + K}\right)^n. \quad (1a,b)$$

When [Rb] is high and $k_+ \gg k_-$,

$$\alpha'_P = \alpha_P \left(\frac{Rb}{L_P + Rb}\right)^m; \beta'_P = \beta_P \left(\frac{T_P}{T_P + Rb}\right)^n. \quad (1c,d)$$

Thus, the relation between opening rate or closing rate and voltage or concentration of activating ion will provide information about the parameters m and n.

Relation Between Change in Relaxation Rates with Voltage and with Activator Ion Concentration

For simplicity we assume that the effective gating charge, z, governing binding to gating sites is the same for open, closed, plugged and unplugged channels. Thus,

$$T_{U,V} = T_{U,0} \exp [zBV]; \qquad L_{U,V} = L_{U,0} \exp [zBV];$$

$$T_{P,V} = T_{P,0} \exp [zBV]; \qquad L_{P,V} = L_{P,0} \exp [zBV];$$

where B = 25.7 mV (e.g., F/RT or e/kT at 25°C). Because z is positive, L and T will become smaller as voltage is made more negative and the gating ions become more effective. Similarly, if isomerization involves the movement of a gating charge a fraction of the way through the membrane field with the opening process governed by an effective gating charge x and the closing rate governed by an effective gating charge y, then the voltage dependence of isomerization can be described as follows:

$$\beta_U = \beta_{U,0} \exp [y_U BV]; \qquad \alpha_U = \alpha_{U,0} \exp [-x_1 BV];$$

$$\beta_P = \beta_{P,0} \exp [y_P BV]; \qquad \alpha_P = \alpha_{P,0} \exp [-x_2 BV].$$

Pennefather et al. (1992) pointed out that in order for the line defining the relation between $\ln(\alpha'_U)$ or $\ln(\beta'_U)$ and voltage to shift in parallel with changes in $\ln(A)$ the following equality must hold,

$$\frac{d \ln (\alpha'_U)}{d \ln (A)} = \frac{d \ln (\alpha'_U)}{B\, dV}. \quad (2)$$

In the Appendix (A9–A11), we show that Eq. 2 implies that,

$$x = \frac{m\,(1 - z)}{1 + (A/L_{U,0})\exp\,[-zBV]}. \tag{3}$$

Thus, for the change of α' with either voltage or concentration to match up, either (a) $z = 1$ and $x = 0$, (*b*) $z = 0$ and $x = m$ $(L_U/(L_U + A)$ or (*c*) z and x are intermediate between these extremes but have values consistent with Eq. 3 (see also, Pennefather et al., 1992). Eq. 3 implies also that if L_U is voltage dependent α'_U will become less voltage dependent at large negative potentials where gating sites become saturated. Because the voltage dependence seems relatively constant over the range ($V_{1/2} \pm 50$ mV) studied in Silver et al. (1994), we have assumed that binding of activator ions is relatively voltage independent (i.e., $z = 0$ and L and T are the same at all potentials). So that, $x = mL_U/(L_U + A)$. Therefore, Eq. 3 predicts that,

$$\frac{d\ln(\alpha'_U)}{d\ln(A)} = \frac{1}{B}\frac{d\ln(\alpha'_U)}{dV} = -m'_U = -m\left[\frac{L_U}{L_U + K}\right] = -x_U. \tag{4a}$$

It can be shown similarly that:

$$\frac{d\ln(\beta'_U)}{d\ln(A)} = \frac{1}{B}\frac{d\ln(\beta'_U)}{dV} = n'_U = n\left[\frac{K}{T_U + K}\right] = y_U; \tag{4b}$$

$$\frac{d\ln(\alpha'_P)}{d\ln(A)} = \frac{1}{B}\frac{d\ln(\alpha'_P)}{dV} = -m'_P = -m\left[\frac{L_P}{L_P + Rb}\right] = -x_P; \tag{4c}$$

$$\frac{d\ln(\beta'_P)}{d\ln(A)} = \frac{1}{B}\frac{d\ln(\beta'_P)}{dV} = n'_P = n\left[\frac{Rb}{T_P + Rb}\right] = y_P. \tag{4d}$$

This also implies that:

$$\alpha'_V = \alpha'_{V1/2}\exp\,[-Bm'(V - V_{1/2})] \tag{4e}$$

and

$$\beta'_V = \beta'_{V1/2}\exp\,[Bn'(V - V_{1/2})]. \tag{4f}$$

Accordingly, if either of the dissociation constants L or T are of the same order of magnitude as the concentration of activator ions, the voltage and concentration dependence of α' and β' will underestimate the level of occupancy that is optimal for isomerization to occur. In the Appendix we show also (see Eq. A14) that, providing Eq. 3 holds, the effective activation and deactivation rates at $V_{1/2}$ (i.e., $\alpha'_{V1/2}$ and $\beta'_{V1/2}$) will remain constant as $V_{1/2}$ changes with V_{rev} (as is observed experimentally).

Rubidium Blockade

Standen and Stanfield (1980) described the voltage dependent blockade of skeletal muscle IR by Rb^+ in terms of a model where Rb^+ binds to a site within the channel (see also Silver et al., 1994). Here we assume that the rate of entry, k_+, into that site is governed by a forward rate constant, k_1, that is relatively voltage independent and is governed by the initial partitioning of Rb^+ into the channel such that $k_+ = k_1[Rb^+]$.

Escape from the plugging site to the outside of the cell involves the movement of the blocking ion over a fraction δ of the membrane field and is governed by a rate constant k_{-1} that increases with depolarization; we assume that k_{-1} contributes most of the voltage dependence of blockade at potentials around $V_{1/2}$. However, because Rb^+ has a small but finite conductance, blockade will be relieved at negative potentials. This escape to the inside of the cell involves movement of the blocking ion over a fraction γ of the membrane field and is governed by a rate constant, k_2 that increases with hyperpolarization; in our models, k_2 contributes most of the voltage dependence of blockade at large negative potentials (i.e., negative to V_{rev} −50 mV). If one assumes firstly, that once one bore of the triple bore channel is plugged the other bores are immediately plugged and secondly, that unplugging of a channel requires the escape of all three of the blocking ions (see above), then the overall unplugging rate $k_- = k_{-1} + k_2$, can be described by the following equation.

$$k_{-,V} = k_{-1.0} \exp [z'BV] + (6.2 \times 10^{18} \text{ ions/coulomb})\, i_{Rb,-90} \exp [-z''B(V + 90)], \quad (5)$$

where $z' = 3\ \delta$, $z'' = 3\ \gamma$, and $i_{Rb,-90}$ is the Rb^+ current in amperes at −90 mV where k_1 is much greater then k_{-1} (i.e., in 160 mM Rb^+). The parameter z' defines empirically the voltage dependence of blockade at potentials around $V_{1/2}$. While z'' defines that voltage dependence at negative potentials where k_- is dominated by escape from the channel to the outside and to the inside of the cell.

Steady State Voltage-activation Curve

Provided that binding of activator ions is fast relative to isomerization, Scheme II can be approximated by a two-state system where all the closed states (C') and all the open states (O') can each be lumped together kinetically. Under those conditions, the voltage-dependence and slope of the voltage-activation curve will be determined by the voltage dependence of the ratio C'/O'. If P_∞ is the steady state open state probability then,

$$P_\infty(V) = \frac{O'(V)}{O'(V) + C'(V)} = \frac{1}{1 + \dfrac{C'(V)}{O'(V)}} = \frac{1}{1 + \dfrac{C'(V_{1/2}}{O'(V_{1/2})} \exp [(V - V_{1/2})/S]} \quad (6)$$

where $V_{1/2}$ is the half-activation voltage and S is the slope-factor defining the steepness of the voltage-activation curve.

In the appendix (Eq. A4) we show that, as expected for a two state system $C'(V)/O'(V) = \beta'(V/\alpha'(V)$.

Thus, under conditions where there is little channel plugging (e.g., when $k_+ \ll k_-$) Eq. 4 predicts that,

$$\frac{C'(V)}{O'(V)} = \frac{\beta'_{U,1/2}}{\alpha'_{U,1/2}} \exp [-B(m'_U + n'_U)(V - V_{U,1/2})] \quad (7a)$$

and when channel plugging predominates (e.g., when $k_+ \gg k_-$)

$$\frac{C'(V)}{O'(V)} = \frac{\beta'_{P,1/2}}{\alpha'_{P,1/2}} \exp [-B(m'_P + n'_P)(V - V_{P,1/2})]. \quad (7b)$$

Thus, as the level of channel plugging (dependent on k_+/k_-) increases, the slope factor, S, which defines the steepness of the voltage-activation curve will change from $1/Bz(m'_U + n'_U)$ to $1/Bz(m'_P + n'_P)$. Furthermore, the relation between S and number of binding sites for activator ions on a channel complex will depend on the level of saturation of those sites in the region of voltages over which the voltage dependence is determined.

Additional Modifications

Silver et al. (1994) observed that in external solutions containing 160 mM Rb^+ values of β' at potentials >20 mV positive to $V_{1/2}$ were smaller than those recorded at the same potential in 160 mM K^+. In the simplest versions of Scheme II*A* and *B*, there should be no difference between those values because K^+ and Rb^+ are assumed to be equieffective in activating the channel and few channels should be plugged at those potentials. It should be emphasized that the prolonging effect of Rb^+ at positive potentials is distinct from the apparent prolongation of open time caused by rapid channel plugging at negative potentials (see Shioya et al., 1993). To accommodate the apparent reduction of β'_U at positive potentials in Rb^+, we assume that this effect is a linear function of the fraction of binding sites for activator ions occupied by Rb^+. With this modification,

$$\beta'_U = \beta'_{U,K} - (\beta'_{U,K} - \beta'_{U,Rb})F. \tag{8a}$$

The effect could arise if Rb^+ had a higher affinity than K^+ for activator sites on open channels. If we assume that the intrinsic isomerization rate β_U is unaffected by replacing K^+ with Rb^+, then combining Eq. 1 and 8a we obtain,

$$(T'_U)^n = (T'_{U,K})^n - [(T'_{U,K})^n - (T'_{U,Rb})^n]F, \tag{8b}$$

where $T' = T/(T + A)$. Of course, the effect also could be explained if the microscopic closing rate, β_U, were dependent on the type of ions occuping the binding sites for activator ions; for example, if the presence of Rb^+ rather than K^+ on a given binding site increased the energy barrier separating closed and open states of the channel. In either case, the rapid exchange of Rb^+ and K^+ at those sites would allow the effect at individual sites to be time averaged and allow the overall effect to be described by a simple equation such as 8. To simplify our simulation we assume that T_P changes in the same manner as T_U so that T_U/T_P is constant at all mole fractions of Rb^+. An effect of Rb^+ on T'_U has consequences for the predicted relation between mole fraction of Rb^+ and the activation rate at $V_{1/2}$. Combining Eq. 8b with A6 one obtains:

$$\beta'_{1/2} = \alpha'_{1/2} = \beta_{U,1/2}(T'_U)^n \frac{1 + \dfrac{\beta_{P,1/2}}{\beta_{U,1/2}}\dfrac{k_1 P}{k_-}}{1 + \dfrac{k_1 P}{k_-}\left(\dfrac{T'_U}{T'_P}\right)^n} \tag{9a}$$

$$= \beta'_{U,1/2} \frac{1 + \dfrac{\beta'_{P,1/2}}{\beta'_{U,1/2}}\overline{P}}{1 + \overline{P}} \tag{9b}$$

where

$$\bar{P} = \frac{k_1 P}{k_-}\left(\frac{T'_U}{T'_P}\right)^n.$$

MATERIALS AND METHODS

Simulations

Schemes II*A* and *B* were simulated using a commercially available software package called Axon Engineer (Axon Software, Newport Beach, OR). This program solves the differential equations implicit in the links between states represented by Schemes II *A* and *B*. It permits the definition of concentration and voltage dependencies of these rates and allows standard stimuli such as simulated voltage-clamp commands to be introduced to mimic actual experiments. Current is calculated by assigning a gating variable ranging from 0 to 1 to each substate. At each integration step the program sums the product of that variable and the predicted probability of the substates. This number is then multiplied by factors that take into account the electrochemical potential (predicted by the Goldman, Hodgkin, Katz equation) and the maximal conductance of the system at 0 mV. The open-unplugged substates were given a gating variable of 1 whereas the plugged-open substates were assigned a gating variable of 0.03 to reflect the relative conductance of those channels. All transitions are considered explicitly, hence the dissociation constants L and T were divided into forward and reverse rate constants by assuming that binding to a given site proceeded at a rate of $[A]10^8$ M^{-1} s^{-1}. In Schemes II *A* and *B*, the plugged-open channels convert to the corresponding unplugged-open substate via two pathways defined by rate constants k_2 and k_{-1}. The program allows for only one pathway between any two substates so that in our simulations the pathways governed by k_2 lead to a dummy substate that decayed immediately (at rate of 10^6/ms) to the corresponding unplugged-open substate. Thus, a total of 21 substates linked via 48 rate constants had to be followed to simulate Scheme II *A* and 38 substates linked via 92 rate constants were followed in simulations of Scheme II *B*. Despite the large number of substates and transitions, the actual number of variables needed to define the schemes (see Table II) were kept small by making simplifying assumptions (see above). Hence, our simplistic algebraic relations could be used to derive the parameters needed for explicit numerical simulations of the schemes.

Experimental Procedures

Experimental procedures were the same as described in the accompanying paper (Silver et al., 1994).

RESULTS

Derivation of Parameters

The relationships described above allow one to use the data presented in the accompanying paper (Silver et al., 1994) to derive the parameters needed to define Schemes II, *A* and *B* and simulate the effects of Rb^+ on gating of IR K channels. However first, a few additional experimental details need to be verified. In many cell types, the voltage activation curve for IR K channels shifts in parallel with $\ln([K]_o)$, if K^+ is the only type of activator ion present (see Silver et al., 1994). Scheme II predicts that a similar parallel shift should be observed if Rb^+ is the only activator ion present. The voltage dependence of steady state IR gating was determined by applying

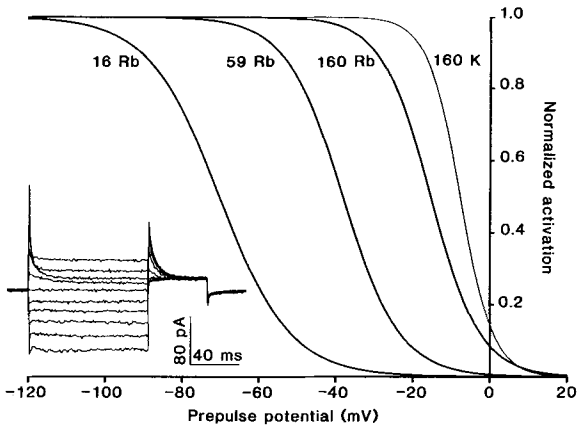

FIGURE 1. Voltage-dependence of macroscopic gating of the IR at different $[Rb]_o$. In all cases intracellular K^+ was around 180 mM. Curves illustrate behaviour predicted from average $V_{1/2}$ and S values (Table I). (*Inset*) Method used to quantify the voltage dependence of gating in 59 Rb^+ + 101 Na^+. From a holding potential of −45 mV prepulses to −95 mV through −5 mV in 10-mV increments are shown, followed immediately by a test pulse to −25 mV. The amplitude of the outward tail current during the test pulse was obtained by fitting with a single exponential. The resulting instantaneous current amplitudes, I_o as a function of the prepulse potential were fitted by nonlinear least squares to:

$$I_o = (I_{o,max} - I_{o,min})/(1 + \exp[(V - V_{1/2})/S] + I_{o,min}.$$

The fitted midpoints, $V_{1/2}$ and slope factors, S are given in Table I, and were used to generate the curves shown here. For comparison, mean data for 160 K^+ are also plotted.

variable prepulses followed by a constant test pulse and measuring the amplitude of the deactivating outward current transient (Fig. 1, *inset;* Fig. 7 of Silver et al., 1994). The results are given in Table I and plotted in Fig. 1. The $V_{1/2}$ values were shifted to more negative potentials as $[Rb]_o$ was lowered and replaced by Na^+, from −16 mV in 160 Rb^+ to −38 mV in 59 Rb^+ and to −70 mV in 16 Rb^+; $V_{1/2}$ was on average 7.3 mV positive to E_{Rb} in 160 Rb^+ (Silver et al., 1994). Assuming that P_{Rb}/P_K is constant at 0.45, a perfect shift of $V_{1/2}$ with E_{Rb} would be to −13 mV, −38 mV, and −71 mV in 160 Rb^+, 59 Rb^+, and 16 Rb^+, respectively. Thus, $V_{1/2}$ appears to shift precisely along with E_{Rb} when $[Rb]_o$ is reduced, comparable to the shift of $V_{1/2}$ with E_K as $[K]_o$ is lowered and replaced by Na^+ (Silver and DeCoursey, 1990). The slope factor appeared to increase as $[Rb]_o$ was lowered, but not enough data exist to be sure of this result. Resolution of current records becomes progressively poorer as the concentration of external gating ion was decreased, limiting the reliability of these data. Because $V_{1/2}$ is −8 mV in 160 mM K^+ we can predict that when only K^+ is present, $V_{1/2}$ will equal 0 mV when external [K] = 218 mM. In 160 mM Rb^+, $V_{1/2}$ is

TABLE I

Steady State Voltage-dependence of IR Gating

$[Rb^+]_o$	$V_{1/2}$	S	n
mM	*mV*	*mV*	
160*	−16.3 ± 2.0	6.16 ± 0.27	6
160	−15.4 ± 2.5	6.48 ± 1.12	4
59	−38.2 ± 1.6	7.48 ± 0.38	7
16	−70.3 ± 5.1	9.34 ± 0.9	2

*Data from Silver et al. (1994). Parameters defined in Eq. 6. Means ± SE are given for n = number of experiment.

−16 mV so that when only Rb^+ is present, $V_{1/2}$ will equal 0 mV when external [Rb] = 298 mM.

Silver et al. (1993) found a slope factor of 4.3 mV for the voltage-activation curve in 160 mM K^+; the slope factor changed to 6.7 mV at high mole fractions of Rb^+. The voltage dependence of the rate of opening α' changed from e-fold/18 mV in 160 mM K^+ to e-fold/26 mV in high mole fractions of Rb^+. This observation implies that the effective gating charges governing α_U and α_P are such that $x_U = 1.4$ and $x_P = 1.0$. The voltage dependence of the rate β' did not change much as the mole fraction of Rb^+ increased, the average for all conditions was e-fold/8.3 mV implying that $y_U = y_P = 3.1$. With Scheme II, the minimal values of m and n consistent with the observed voltage dependence are $m = 2$ and $n = 4$. However, if the binding sites governing gating are significantly occupied in the range of potentials around $V_{1/2}$, that is if L, T, and A are of the same order of magnitude, the parameters m and n will be underestimated from the voltage dependence of the steady state level of activation and of the kinetics of activation and deactivation. Because we have no independent estimate of m and n, we derived the parameters that define our model for $m = 2$, $n = 4$ and for $m = 3$, $n = 9$ (Scheme II, A, and B, respectively).

As a point of reference, we present the value of parameters for the condition where $V_{1/2} = 0$ mV. Eq. 4 predicts that $m'_U = m[L_U/(L_U + A_U)] = x_U = 1.4$ in the absence of Rb^+ and that when the Rb^+ mole fraction is high, $m'_P = m[L_P/(L_P + A_P)] = x_P = 1.0$. Inserting the values of m and A we can derive the values of $L_{U,K}$ and $L_{P,Rb}$ at $V_{1/2} = 0$ mV. Once those values have been established, the intrinsic isomerization rates of opening of unplugged and plugged channels can be derived from the extrapolated value of $\alpha'_{1/2}$ at 0 mV in the presence of a concentration of gating ion that sets $V_{1/2} = 0$ mV (i.e., A_U or A_P). In the absence of Rb^+, $\alpha_{U,0}(A_U/(L_U + A_U)^m = \alpha'_{1/2} = 0.2$/ms. At a high mole fraction of Rb^+, $\alpha_{P,0}(A_P/(L_P + A_P))^m = \alpha'_{1/2} = 0.025$/ms. Similarly, Eq. 4 predicts that $n'_U = n(A_U/[T_U + A_U)] = y_U = 3.1$ and $\beta_{U,0}[T_U/(T_U + A_U)]^n = \beta'_{1/2} = 0.2$/ms in the absence of Rb^+. At a high mole-fraction of Rb^+, $n'_P = n[A_P/(T_P + A_P)] = y_P = 3.1$ and $\beta_{P,0}[T_P/(T_P + A_P)] = \beta'_{1/2} = 0.025$/ms. Values of α, β, T, and L deduced from these relations are given in Table II. The values of T_P and L_P are likely to be slightly underestimated since we have assumed that all of the channels are plugged at potentials around $V_{1/2}$ in 160 mM Rb^+.

As mentioned above, there appears to be a slowing of β' as the Rb^+ mole-fraction increases. To quantify this effect we averaged the values for the voltage dependence of β' (presented in Table II of Silver et al., 1994) to derive a best estimate of $y_U = 3.1$. Using this value to extrapolate $\beta'_{U,1/2}$ (0.2/ms at −8 mV) and $\beta'_{P,1/2}$ (0.025/ms at −16 mV) to their predicted values at potentials where β' is dominated by the behavior of unplugged channels, we estimate that $\beta'_{U,K}/\beta'_{U,Rb} = 3.2$ at + 5 mV. The effect appears to be a linear function of F as implied by Eq. 8 because, in solutions containing 80 mM Rb^+ + 80 mM K^+ where $F = 0.5$, β' at +5 mV is half-maximally shifted between β'_K measured when $F = 0$ and β'_{Rb} measured when $F = 1$ (data not shown). The magnitude of the effect can be explained if $T_{U,K}/T_{U,Rb} = 1.5$ (because Eq. 1b predicts that $(T'_{U,K}/T'_{U,Rb})^n = 3.2$ when $T_{U,K}/T_{U,Rb} = 1.5$). To simplify the simulation we have assumed also that $T_{P,K}/T_{P,Rb} = 1.5$. Closed channels may also have a higher affinity for Rb^+ but this cannot be determined directly from our data. As that assumption makes little difference to the ability of our simulations to match currently available data, this added complication was not included in our model.

TABLE II

Summary of Parameters Derived for Scheme II

Scheme IIA				Scheme IIB			
m	= 2*	n	= 4*	m	= 3*	n	= 9*
x_U	= 1.4	y_U	= 3.1	x_P	= 1.4	y_U	= 3.1
x_P	= 1.0	y_P	= 3.1	x_U	= 1.0	y_P	= 3.1
$L_{U,K}$	= 520 mM	$T_{U,K}$	= 63 mM	$L_{U,K}$	= 193 mM	$T_{U,K}$	= 306 mM
$L_{P,K}$	= 298 mM*	$T_{P,K}$	= 130 mM*	$L_{P,K}$	= 149 mM*	$T_{P,K}$	= 627 mM*
$L_{U,Rb}$	= 520 mM*	$T_{U,Rb}$	= 44 mM	$L_{U,Rb}$	= 193 mM*	$T_{U,Rb}$	= 204 mM
$L_{P,Rb}$	= 298 mM	$T_{P,Rb}$	= 87 mM	$L_{P,Rb}$	= 149 mM	$T_{P,Rb}$	= 418 mM
α_U	= 2.3/ms exp[$-x_U$BV]	β_U	= 79/ms exp[y_UBV]	$\alpha_{U,K}$	= 1.3/ms exp[$-x_U$BV]	$\beta_{U,K}$	= 25/ms exp[y_UBV]
α_P	= 0.10/ms exp[$-x_P$BV]	β_P	= 9.6/ms exp[y_PBV]	α_P	= 0.084/ms exp[$-x_P$BV]	β_P	= 0.77/ms exp[y_PBV]
z''	= −0.4	z'	= 2.4	z''	= −0.4	z'	= 2.4
$k_{1,Rb}$	= 67/mM/ms	$k_{-1,Rb}$	= 1287 exp[z'BV]/ms	$k_{1,Rb}$	= 67/mM/ms	$k_{-1,Rb}$	= 1287 exp[z'BV]/ms
$k_{2,Rb}$	= 116 exp[z"BV]/ms	P_{Rb}/P_K	= 0.45	$k_{2,Rb}$	= 116 exp[z"BV]/ms	P_{Rb}/P_K	= 0.45

*Parameters not defined by data of Silver et al. (1994).

In 160 mM Rb^+ and with a −90 mV driving force the rate of reversal of channel plugging, k_-, is dominated by the rate of escape of Rb^+ from the channel via the cytosolic mouth, k_2. At that potential k_- and hence k_2 are reflected in a single channel conductance estimated to be 0.7 pS and which corresponds to an ionic flux of 470/ms at −90 mV. This escape rate should be independent of the external concentration of Rb because it assumes prior occupancy of the channel plugging site. Because $k_+ = k_-$ when the channel is plugged 50% of the time and channel blockade produced by Rb^+ is half-maximal in 7 mM Rb^+ at −90 mV (see Silver et al., 1994), $k_1 = k_+/7$ mM = 470/ms/7 mM = 6.7×10^7/M/s. This rate is typical of channel plugging reactions by small molecules and ions (see Pennefather and Quastel, 1980). The steady state level of blockade decreased with hyperpolarization below −90 mV, ~e-fold/65 mV (data not shown). If we assume that k_1 is voltage independent, this implies that z'', the effective gating charge governing the voltage dependence of k_2, is such that $z'' = -0.4$ (see also Standen and Stanfield, 1980) and that $k_{2,V}$ = (116/ms) exp[−0.4BV].

To derive k_- at 0 mV where it is dominated by k_{-1}, we consider the concentration of P that causes the fraction of activated channels at 0 mV to change from 50% to 25% ($[P]_{(1/2,0)}$); this implies that C'/O' changes from 1 to 3 (see Eq. 6). We assume that the position of the activation curve and the reversal potential are not affected much by this concentration of P (true for [Rb] ≤ 20 mM) and that the current through open plugged channels is negligible at 0 mV. By combining Eq. A3d and A3e of the appendix one obtains the following relation defining k_-,

$$3 = 1 + \frac{\alpha_U}{\beta_U}\frac{[Rb]_{(1/2,0)}k_1}{k_-}\left\{\frac{\beta_P}{\alpha_P}\left(\frac{L_P + A}{L_U + A}\right)^m + \left(\frac{T_U}{T_P}\left(\frac{T_P + A}{T_U + A}\right)\right)^n\right\}$$

hence,

$$k_- = k_1\frac{\alpha_U}{\beta_U}\frac{[Rb]_{(1/2,0)}}{2}\left\{\frac{\beta_P}{\alpha_P}\left(\frac{L_P + A}{L_U + A}\right)^m + \left(\frac{T_U}{T_P}\left(\frac{T_P + A}{T_U + A}\right)\right)^n\right\} \quad (10)$$

Eq. 10 takes into account the two effects of Rb^+ to inhibit the IR current: (*a*), channel plugging per se and (*b*), modification of the stability of both open- and closed-plugged channels. Silver et al., (1994) found that $[Rb]_{1/2,0}$ is ~20 mM. Inserting our derived parameters for $\alpha_{U,0}$, $\beta_{U,0}$, $\alpha_{P,0}$, $\beta_{P,0}$, $L_{U,K}$,$L_{P,K}$, $T_{U,K}$, $T_{P,K}$ (see Table II) one obtains a value of k_-/k_1 = 21 mM. Therefore, because $k_1 = 6.7\text{x } 10^7$/M/s, we deduce that k_- = 1,403/ms. Because $k_- = k_{-1} + k_2$ (see Eq. 3) and we have decided previously that k_2 = 116/ms at 0 mV and $z'' = 2.4$, we can deduce that $k_{-1,Rb}$ = (1,287/ms) exp[2.4BV]. A value of k_-/k_+ = 20 mM would be expected if only blockade of open channels were responsible for the reduced conductance without any change in gating parameters (e.g., if α, β, L and T were not affected by channel plugging). However, modification of the kinetics of IR gating by Rb^+ suggest that gating parameters are affected. The effect of plugging by Rb^+ to modify activator ion affinity (changes in L and T) appears to be offset by changes in the intrinsic isomerization rates (α and β).

Additional Constraints Due to IR Kinetics at $V_{1/2}$

The change of $\alpha'_{1/2}$ with F depicted in Fig. 13 of Silver et al. (1994), provides an additional constraint on the parameters used in our simulations. Eq. A7 of the

Appendix predicts that when half of the channels are plugged, $\alpha'_{1/2}$ should be reduced half of the way to the value expected when all of the channels are plugged. Because $[Rb]_{1/2,0}$ = 20 mM, a concentration of 8–12 mM would be expected to cause this half-maximal shift given that $V_{1/2}$ = −12 mV in 20 mM Rb^+/140 mM K^+ and assuming neither T_P nor T_U changed with F. Experimentally however, a concentration of 40 mM appears to be required to cause such a shift. When we set $T_{U,K}/T_{U,Rb}$ = $T_{P,K}/T_{P,Rb}$ = 1.5, the discrepancy is reduced (see Fig. 2). This observation provides additional justification for allowing Rb^+ to have a higher affinity then K^+ for the allosteric binding sites for activator ions on open and open-plugged channels (see above).

As discussed above, and in the Appendix, a simple two state system would give rise to equal values of α' and β' at $V_{1/2}$. However, Silver and DeCoursey (1990) and Silver et al. (1994) have estimated that the value of $\beta'_{V,1/2}$ was half that of $\alpha'_{V,1/2}$ in 160 mM

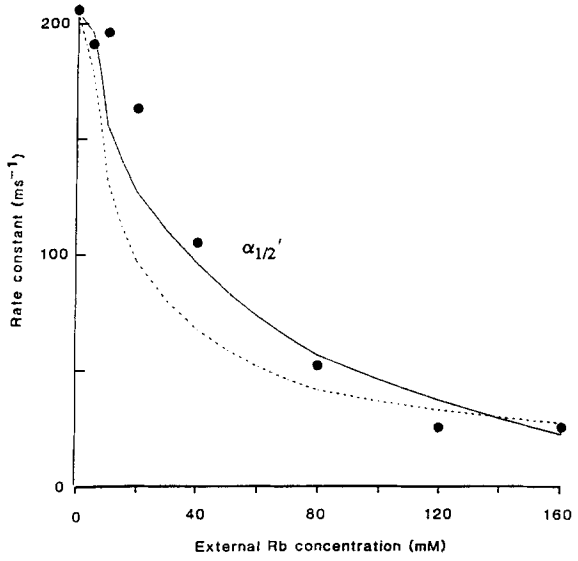

FIGURE 2. Effect of Rb^+ on the activation rate at $V_{1/2}$ (α'). Solid dots are experimental data taken from Fig. 13 of Silver et al. (1994). Dashed line is based on Eq. 9 assuming that the affinity of open channels for Rb^+ is the same as for K^+. Solid line is the predicted relation if T'_U and T'_P are allowed to change according to Eq. 8*b* with $T_{U,K}/T_{U,Rb}$ = $T_{P,K}/T_{P,Rb}$ = 1.5. Allowing the affinity of Rb^+ for open channels to be higher than that of K^+ improves the agreement between predicted and experimental results.

K^+. This discrepancy can be accommodated in Scheme II if K^+ itself has some ability to plug IR channels (e.g., it has a significant dwell time in the channel as it permeates). If the binding sites for activator ions on a channel plugged by K^+ are modified to the same extent as those on channels plugged by Rb^+ then Eq. 9 predicts that the actual deactivation rate, $\beta'_{1/2}$, will be related as follows to the extrapolated estimate of that rate, $\beta'_{U,1/2}$, reflecting mostly unplugged channels,

$$\frac{\beta'_{1/2}}{\beta'_{U,1/2}} = \frac{\left[1 + \frac{\beta_{P,1/2}}{\beta_{U,1/2}} \frac{k_I[K]}{k_-}\right]}{1 + \frac{k_I[K]}{k_-}\left[\frac{T'_U}{T'_P}\right]^n}. \tag{11}$$

Although k_- at 0 mV will be considerably larger for K^+ than for Rb^+, it is possible that in 160 mM K^+, $k_I[K^+]$ might be sufficient for a significant level of occupancy of

the channel pore to exist at $V_{1/2}$. If this occupancy of the channel by K^+ reduces the affinity of activator ion binding sites on open channels in the same manner as Rb^+, it will cause the actual $V_{1/2}$ to shift to a value more negative than expected from the values of β' at positive potentials and produce the apparent discrepancy between the extrapolated $\beta'_{1/2}$ and $\alpha'_{1/2}$. The rate α' need not be distorted in this manner if channel occupancy is relatively constant between $V_{1/2}$ and $V_{1/2}$ −50 mV (see Silver et al., 1994). Eq. 11 predicts that the expected value of β' will be less than the extrapolated value provided that,

$$\frac{\beta_{P,1/2}}{\beta_{U,1/2}}\left(\frac{T_P\,(T_U + K)}{T_U\,(T_P + K)}\right)^n = \frac{\beta'_{P,1/2}}{\beta'_{U,1/2}} < 1,$$

in other words provided that the channel occupied by K^+ closes more slowly than an unoccupied channel. This seems likely because channel blockade appears to slow channel closing (see Shioya, Matsuda, and Noma, 1993). It is difficult to interpret this effect further because of a lack of hard data regarding the influence of channel occupancy by K^+ on L and T. A more direct measure of occupancy would be useful in determining that effect. This might be obtained by looking for a competitive effect of $[K^+]$ on the channel plugging action of a fixed concentration of Rb^+ (see Neyton and Miller, 1988). Such an effect would be expected to reduce $k_{1,Rb}$, leading to reduced blockade by Rb^+ as $[K^+]$ is increased (see Standen and Stanfield 1980). Because of the uncertainty surrounding the possible channel plugging actions of K^+, we make no attempt to incorporate this effect into our simulations.

Simulated Results

The following simulations were generated using a computer program called "Axon Engineer" that is designed to simulate the dynamics of cellular ionic signals (see Materials and Methods). The simulations are based on Scheme II *A* and use the parameters presented in Table II for that scheme. Essentially identical results were obtained with the set of parameters derived for Scheme II *B* and also presented in Table 2.

In Fig. 3 A we reproduced the results depicted in Fig. 1 of Silver et al. (1994) that illustrate the effect of increasing Rb mole-fraction on steady state responses to ramps of voltage. The ramp is illustrated in the bottom panel. Currents, in increasing order of magnitude at −100 mV, are those predicted for mole fractions of 0, 0.031, 0.125, and 0.5. The last line represents the leak current included in the simulation. Because endothelial cells used by Silver et al. (1994) had a capacitance of 10–15 pF, the current densities (in $\mu A/cm^2$) plotted here can be converted to absolute current through multiplication by $1–1.5 \times 10^{-7}$ cm^2. The parameters for Scheme II *A*, derived primarily from kinetic data, predict the steady state effects of Rb^+ very well. The top panel plots the summated and normalized activity (equivalent to normalized conductance) of all the substates considered in the simulation. It is clear that the Rb^+ blockade decreased steeply with depolarization positive to −50 mV. Below −50 mV the blockade is less voltage dependent and is reduced rather than increased by hyperpolarization. These results are very similar to those described by Standen and Stanfield (1980).

Fig. 3 *B* illustrates the results of the same simulation as in Fig. 3 *A* but plotted with

a higher gain. Results for mole fraction of 0, 0.125, 0.5, and 1 are depicted. In our simulations we distinguished between the effective concentration of permeating ions ([G]) and of activator ion ([A]). As the Rb^+ mole-fraction increased, we reduced [G] to reflect the lower permeability of Rb^+ e.g., [G] = 72 mM in 160 mM Rb^+ because $P_{Rb}/P_K = 0.45$. Internal K^+ was set at 180 mM so that the reversal potential shifted from −2 to −26 mV as the mole-fraction increased from 0 to 1 (see Silver et al., 1994). However, because the midpoint of the voltage-activation curve shifted by only 8 mV and because Rb^+ blockade is steeply voltage dependent the peak outward current paradoxically increases as blocking ion concentration increases.

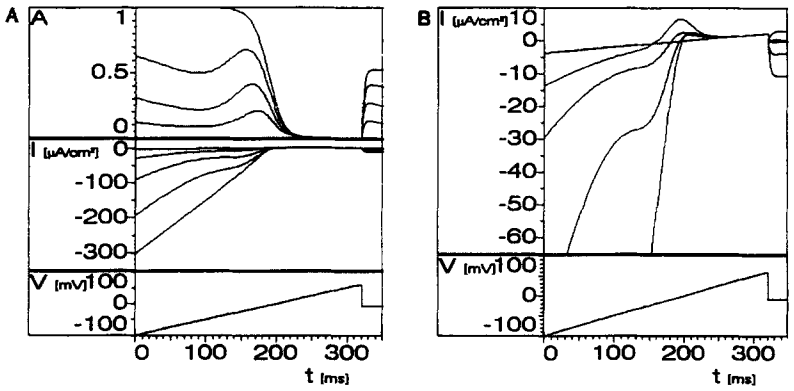

FIGURE 3. Simulation of the effects of Rb^+ on the response to ramps of the voltage clamp command voltage. The protocol is the same as used to generate the experimental results depicted in Fig. 1 of Silver et al. (1994). (*A*) The bottom shows the voltage ramp. The middle shows the simulated currents for the condition 0, 5, 20, and 80 mM Rb^+ with 160 mM of total activator ion. The shallowest line represents the linear leak current that was also considered in our simulations. The top displays the corresponding open state activity of the channel responsible for the currents shown in the middle. This activity is the sum of the probability of all open substates multiplied by the relative conductance of those substates. Whole cell current is then predicted from the Goldman, Hodgkin, Katz equation and a maximum permeability value for the current. Parameters used in the simulation were those presented in Table II. T'_U and T'_P were changed according to Eq. 8*b* assuming $T_{U,K}/T_{U,Rb} = T_{P,K}/T_{P,Rb} = 1.5$. (*B*) Same current records as in *A* but at 5× gain.

Fig. 4 shows that our model is versatile enough to account for the various effects of increasing Rb^+ mole fraction on the kinetics of IR. These simulations reproduce almost exactly the results depicted in Fig. 7 and 8 *b* of Silver et al. (1994). In most of our simulations, a linear leak was assumed. However in Fig. 4 *C*, for the simulation involving a test pulse the +17 mV, the leak was increased to mimic the nonlinear leak observed experimentally in that region of membrane potentials (see Silver et al., 1994).

In Fig. 5 we simulated the effect of lowering intenal K^+ on Rb^+ blockade as probed using voltage-clamp ramps (see Fig. 2, Silver et al., 1994). To reproduce those experimental results, three of the parameters used to describe the results when K_i was

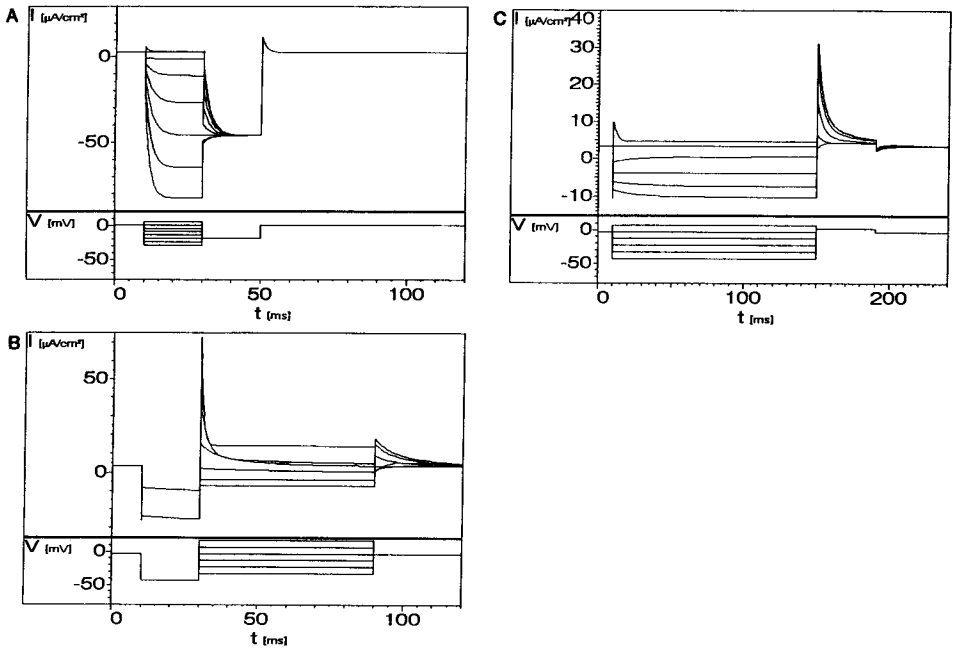

FIGURE 4. Simulations of voltage-clamp protocols used by Silver et al., (1994) to describe the kinetics and voltage-activation curves of IR channels. (*A*) 160 K^+, 0 Rb^+; protocol identical to that used in Fig. 7 (*left inset*) of Silver et al., (1994). (*B*) 160 Rb^+, 0 K^+; protocol in Fig. 7 (*right inset*) of Silver et al. (1994). (*C*) 160 Rb^+, 0 K^+; protocol in Fig. 8 *b* of Silver et al. (1994). Parameters used in the simulations are those tabulated in Table II. (*C*) The trace representing the response to a test pulse of +17 mV the leak conductance was increased threefold to reflect the outward rectification of the leak conductance observed experimentally.

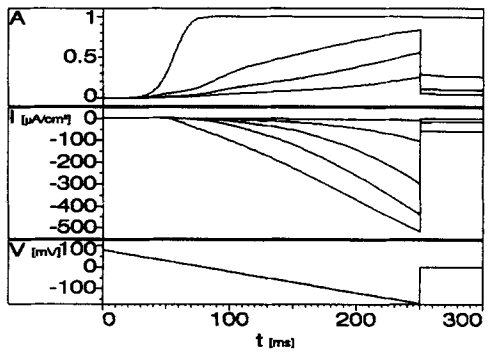

FIGURE 5. Simulations of the effect of low internal K^+. Protocol is identical to that used in Fig. 2 of Silver et al. (1994). Bottom shows ramp used to activate currents. Middle shows the simulated current in 0, 5, 20, and 80 mM Rb^+ with 160 mM of total activator ion. Shallowest trace shows leak current. Top shows channel activity corresponding to the current traces. GHK rectification is assumed. Internal K^+ is set at 40 mM. To simulate the +36-mV shift in the activation curve of IR observed by Silver et al. (1994) when intracellular K^+ is reduced, all values of T and L are reduced fourfold from those deduced for the normal internal K^+ condition (see Table II). To mimic the enhanced Rb^+ blockade around $V_{1/2}$, k_{-1} is reduced 1,750-fold.

normal had to be modified; T and L had to be reduced by a factor of 4 and k_{-1} had to be reduced by a factor of 1,750. In the experiments of Silver et al. (1994) intracellular K^+ was reduced by recording IR using K^+-free recording pipettes. The reversal potential was shifted to +40 mV suggesting that $[K^+]_i$ was only reduced to 40 mM; significant influx of K^+ into the cell presumably balances the loss of K^+ into the patch pipette. The voltage-activation curve of IR appears to shift in parallel with E_K even when E_K is reduced by reducing internal K^+ (Silver and DeCoursey, unpublished results). In our simulations, this effect was reproduced by reducing T and L by the same factor that internal K^+ was reduced (in this case by a factor of 4). When internal K^+ is low, the potency for blockade of the IR by Rb^+ appears to be greatly enhanced around 0 mV, while the potency is the same as with normal internal K^+ at potentials negative to −50 mV. This effect was simulated by reducing k_{-1} while leaving k_2 unchanged. The effect suggests that internal K^+ can interact with Rb^+ ions that enter the channel from the outside to block the channel in such a way that increases the rate at which Rb^+ leaves the channel via the "external" mouth (i.e., increases k_{-1}).

DISCUSSION

In this paper, we have attempted to demonstrate the versatility of an ion-activated channel model of IR gating by using it to develop an explanation for the multiple effects on IR channel gating of replacing external K^+ by Rb^+. In this model isomerization between open and closed states of the IR channel is allosterically modulated by occupancy of binding sites for K^+ and related activator ions. Occupancy of some of those sites promotes channel opening while occupancy of other sites stabilizes the open state. Thus, the rates of both opening and closing will be a function of both voltage and ion concentration. If the change in occupancy of those sites with concentration of activator ions (A) matches the change in occupancy with voltage then the voltage dependent gating properties of such a channel will shift in parallel with ln ($[A]$) and hence with E_A, as is observed with the IR channel. With such models, because occupancy of the binding sites and level of activation are linked, the voltage dependence of gating could conceivably arise from either voltage dependent isomerization between open and closed states, voltage dependent binding of activator ions, or a combination of voltage dependencies of these two processes. Here we have simply focused on the first possibility, but similar results are obtained if only binding or both binding and isomerization are allowed to be voltage-dependent.

If occupancy of the channel pore by a permeating activator ion is allowed to influence the affinity of the allosteric binding sites for activator ions then it becomes quite straightforward to use the ion-activated channel model to account for the many effects of Rb^+ and Rb^+/K^+ mixtures on IR channel gating. Moreover, these effects can be related to the fraction of channels plugged by Rb^+. The simplest implementation of this model, in which external K^+ and Rb^+ interact with the allosteric modulatory sites in exactly the same manner and differ only in their permeation properties, could not account for all the experimental observations. However allowing the affinity of Rb^+ for those sites to be 1.5-fold greater than that of K^+, greatly improved the predictive utility of the model (see Fig. 2). Support for the increased potency of Rb^+ also comes from the observation that the decay rate is slowed in external solutions containing 160 mM Rb^+ at positive potentials where the

channel pore will be occupied mostly by internal K^+ whereas the activator sites will be occupied by Rb^+. At those potentials the rate of deactivation is slowed over that recorded at the same potentials in 160 mM K^+ (see Silver et al., 1994).

Although a few arbitrary decisions had to be made in setting up our simulations, such as choosing the number of allosteric sites on the channel and assigning all of the voltage dependence of gating to the isomerization step, once those decisions were made all of the parameters needed to define our model were constrained by the data of Silver et al. (1994). These decisions did not affect our basic conclusions that the ion activated channel model is robust enough to account for the actions of K^+, Rb^+, and Rb/K^+ mixtures on IR channel gating. It is possible that other ions may bind to the allosteric sites and activate IR channels, such as Tl^+ (Hagiwara, Miyazaki, Krasne, and Ciani, 1977; Stanfield, Ashcroft, and Plant, 1981) and perhaps Cs^+ (Mitra and Morad, 1991; Carmeliet 1992). A rough sequence of potency of $Cs^+ > Rb^+ > K^+$ can be inferred from that data but needs to be verified explicitly. This contrasts with the permeation sequence of $Tl^+ > K^+ > Rb^+ > NH_3^+ > Cs^+$ (Hagiwara and Takahashi, 1974) and the similar sequence for activation of the rat brain K channel known as RCK4 (Pardo, Heinemann, Terlau, Ludewig, Lorra, Pongs, and Stuhmer, 1992).

An early version of the ion activated channel model of IR channel gating was proposed by Horowicz, Gage, and Eisenberg (1968). Based in part upon the increased K^+ efflux resulting from increased $[K^+]_o$, they proposed that the IR conductance was activated by association of two K^+ ions with control sites on each membrane transporter accessible only from the extracellular side of the membrane. Ciani, Krasne, Miyazaki, and Hagiwara (1978) proposed a detailed model in which several K^+ ions from the external solution bind to sites linked to the IR channel, but separate from the permeation pore. Pennefather et al. (1992) proposed a model of this class for I_{K1} in cardiac myocytes, in which intrinsic isomerization rates of the channel are regulated by occupancy of allosteric binding sites for activator ions. Because those sites are accessible when the channel is closed they are likely to be distinct from binding sites governing channel permeation. In this paper, we have described a modification of that allosteric model that allows channels that are plugged by Rb^+ to close and to have different affinities for gating ions than unplugged channels.

An alternative model that the voltage-dependence of the IR might be due to an intracellular cationic blocking molecule was first suggested on the basis of similarities between the IR and delayed rectifier K^+ currents after addition of intracellular quaternary ammonium ions (Armstrong, 1969). The dependence of the IR on external K^+ might reflect block of the channel by an intracellular cation, with the blocker being knocked out of the channel at potentials negative to E_K by K^+ influx (Armstrong, 1969; Hagiwara and Takahashi, 1974; Hille and Schwarz, 1978). When this proposal was first made, the IR conductance was thought to be time-independent. Subsequently, IR gating was found to have a distinct time dependence which shifted along with E_K (Almers, 1971; Hagiwara et al., 1976); but this property still could be explainable by a time- and voltage-dependent ionic block. The discovery that outward currents through I_{K1} channels of cardiac myocytes are sensitive to block by intracellular Mg^{2+} (Vandenberg, 1987; Matsuda et al., 1987), raised the possibility

that Mg^{2+} might be the gating particle for some IR channels. However, it is now clear that a time-dependent gating of the IR K channels which is distinct from Mg^{2+} block occurs in various tissues (Matsuda et al., 1987; Matsuda, 1988; Ishihara et al., 1989; Silver and DeCoursey, 1990; Burton and Hutter, 1990; Oliva et al., 1990). The voltage dependence of I_{K1} block by Mg^{2+} is much weaker with an effective gating charge of 1.14 (Matsuda, 1991), than is the voltage dependence of IR gating which appears to be governed by an effective gating charge ranging from 3.1 to 5.9 (Leech and Stanfield, 1981; Tourneur, Mitra, and Rougier, 1987; Cohen et al., 1989; Burton and Hutter, 1990; Silver and DeCoursey, 1990; Silver et al., 1994). Moreover, Mg^{2+} blockade appears to develop and recover essentially instantaneously after voltage steps under conditions where well-resolved time-dependent gating also is observed (Ishihara et al., 1989). The voltage dependence of the time constants of those voltage-jump relaxations predicts the voltage dependence of the steady state level of IR (see Ishihara et al., 1989; Silver and DeCoursey, 1990; Pennefather et al., 1992). The principle gating of IR K-channels thus appears to be the result of a voltage-dependent isomerization or conformational change between open and closed states of the channel.

An IR channel recently has been cloned (Kubo et al., 1993) which when expressed in oocytes exhibits many properties in common with the IR channel in endothelial cells. The relatively small protein subunit (428 AA) generated by the IRK1 gene does not contain an S-4 type transmembrane sequence (that sequence is enriched in positively charged residues which appears to contribute to voltage detection in many voltage-gated K channels, see Liman, Hess, Weaver, and Koren, 1991). The IRK1 channel sequence appears to contain two transmembrane regions linked by a hydrophilic region that exhibits considerable sequence homology with the 'P region' linking the fourth and fifth transmembrane region of voltage-gated K channels such as the *Shaker* type K channel (Kubo et al., 1993). There is considerable evidence now that the P-region of four equivalent subunits combine to form the ion pore of *Shaker* type K channels (MacKinnon, 1991).

Lee (1992) has proposed that voltage dependent gating of K^+ channels of the *Shaker* type and other related channels occurs because the 'P' region of each of the four channel subunits contains a highly conserved tyrosine residue (Y_{445}) that in the closed state is coordinated through hydrogen bonds with corresponding tyrosines in the other subunits lining the channel. Opening would involve a disassembly of this complex through electron transfer to a nearby tryptophan (W_{434} or W_{435}). The voltage sensor in that model is an aspartate (D_{447}) in *Shaker,* which is postulated to promote electron transfer as it is moved towards Y_{445} through the influence of a depolarizing field. A similar model might account for voltage dependent gating of the IRK1 channel (Lee, personal communication). The P region of the IRK1 channel sequence also contains a tyrosine (Y_{145}) in a position analogous to Y_{445} of *Shaker.* The residue analogous to D_{447} is a neutral phenylalanine whereas a glutamate residue (E_{138}) is found nearby but on the putative cytoplasmic side of the conserved Y_{145}. As a working hypothesis, using our ion-activated channel model, movement of the P region during opening may expose the negatively charged E_{138} to the external solution where it may serve to enhance the binding of activator cations and lead to stabilization of the open state. Occupancy of other ion binding sites on the closed

channel might promote channel opening. It is notable that the P region of RCK4 contains a K^+ binding site that is accessible in closed channels and must be occupied if that channel is to be activated (Pardo et al., 1992). Hence, the negatively charged cysteine (C_{149}) found in the analogous region in IRK1 may play a role in regulating the opening of IR K-channels. These proposals obviously are highly speculative, but could be tested by site-directed mutagenesis experiments. Experience with the effects of site directed mutagenesis on the permeation and binding of cations to the P region of other K channels suggests that multiple residues can influence the absolute and relative affinities of cation binding sites (see Kirsch, Drewe, Taglialatella, Joho, Debiasi, Hartmann, and Brown, 1992).

Multi-ion pores and single filing vs coupled parallel bores. A large body of evidence suggests that the independence principle does not apply to ion permeation through IR channels and that multiple interacting ions can pass through a given IR channel simultaneously (see Hille and Schwarz, 1978). One way of describing this interaction is to propose a model in which ions permeate the channel by hopping over energy barriers separating sequential binding sites (energy wells) but that those ions cannot pass each other. This single-file movement of multiple ions through the channel allows for interactions between permeating ions due charge repulsion (see Hille and Schwarz, 1978). Models of this type can reproduce general features of steep voltage-dependent ionic block, anomalous mole fraction effects, high unidirectional flux ratios, and the $E-E_K$ dependence of IR currents. However problems with single-file models have been noted and alternative models suggested (see Draber, Schultze, and Hansen, 1991).

Single-channel data now suggest that several types of channels may be composed of multiple pores which may function independently under some circumstances, but which sometimes gate cooperatively (in a concerted all-or-none manner) (Hanke and Miller, 1983; Krouse, Schneider, and Gage, 1986; Matsuda, 1988). The binding sites within the channel that govern permeation in these parallel pathways might also interact. Indeed, "correlated ion flux through parallel pores" provides an alternative, allosteric model that may be as versatile as "multi-ion, single file pore" models in reproducing the various electrophysiological properties of IR channels (see Berry and Edwards, 1993). Our suggestion that occupancy of the parallel bores by Rb^+ is a concerted cooperative reaction is consistent with correlated flux models of permeation. As pointed out here, such models also allow Rb^+ blockade to be steeply voltage dependent even if each bore contains a single blocking site for Rb^+, ~80% into the membrane field (see Kirsch et al., 1992). The parallel bore model also multiplies the number of equivalent allosteric sites that can be associated with a channel complex by increasing the number of equivalent subunits that would be required to combine to form the macromolecular channel complex. Although there need not be multiple ions within a given bore, allosteric binding sites on the outside of the channel may influence permeation just as they modulate gating. The concentration of internal K^+ appears to influence the permeation of external Rb^+ (this study) and external K^+ appears to influence the potency of internal Mg^{2+} to block the channel (see Oliva et al., 1990; Matsuda, 1991).

Permeant ion effects on gating of other channels. The gating kinetics of a number of ion channels are influenced by the species of ion present or carrying current. These

effects have been interpreted in two main ways: (*a*) direct interference with channel closure by permeating ions or (*b*) an indirect allosteric modulation of that process. In support of the first mechanism, an inverse relationship has been observed between the lifetime of the open channel and the single channel conductance when ion species or concentration is varied (Kolb and Bamberg, 1977 [gramicidin]; Van Helden, Hamill, and Gage, 1977; Ascher, Marty, and Neild, 1978 [endplate channels]; Benneton and Christophersen, 1990 [red cell Ca^{2+} activated K^+ channels]); less permeant ions are presumed to reside longer within the channel during permeation. This idea is supported by the observation of certain channel blockers which preferentially bind to open channels also inhibit channel closing (Armstrong, 1971 [squid delayed rectifier]; Neher and Steinbach, 1978 [endplate channels]; Demo and Yellen, 1992; and Miller, Latorre, and Reisin, 1987 [maxi-K^+ channels]; Shioya et al., 1993 [I_{K1}]). As a counterexample, in the absence of external permeant ions, occupancy of the maxi-K channel by Na^+ or Ba^{2+} stabilizes the closed state (Neyton and Pelleschi, 1991).

On the other hand, other types of evidence points to allosteric mechanisms that postulate modulatory binding sites for permeant ions on or near channels. The kinetics of Amphotericin B channels depend on the species and concentration of ions present but not on the species carrying current (Ermishkin, Kasunov, and Potseluyev, 1977). Adams, Nonner, Dwyer, and Hille (1981) found no correlation between channel occupancy and open-time of endplate channels, after testing a wide variety of permeant cations. Voltage-independent effects of permeant ions on the open-time of stretch-activated channels were interpreted in terms of an allosteric site outside the permeation path (Yang and Sachs, 1990). The failure of permeant ion concentration to effect K^+ channel closing, the lack of correlation between the conductance of an ion species and its effects on gating, and discrepancies between the effects of Rb^+ on conductance and on deactivation kinetics of lymphocyte K^+ channels was interpreted as evidence for a modulatory site in the external vestibule of that channel (Shapiro and DeCoursey, 1991). Thus, a modulatory role for ions on gating properties effected through allosteric sites may be a property shared by many types of K channels.

APPENDIX

Equilibrium Relations

At equilibrium Scheme II predicts the following equalities:

$$C_U A_m = \left(\frac{A}{L_U + A}\right)^m C_T; \qquad O_U A_m = \left(\frac{T_U}{T_U + A}\right)^n O_T;$$

$$C_P A_m = \left(\frac{A}{L_P + A}\right)^m C_{TP}; \qquad O_P A_m = \left(\frac{T_P}{T_P + A}\right)^n O_{TP};$$

$$\alpha_U C_U A_m = \beta_U O_U A_m; \qquad \alpha_P C_P A_m = \beta_P O_P A_m;$$

$$O_P A_m = \frac{k_1 P}{k_-} O_U A_m; \qquad C_P A_m = \frac{\alpha_U}{\beta_U}\frac{\beta_P}{\alpha_P}\frac{k_1 P}{k_-} C_U A_m.$$

Steady State Predictions

If g is the fractional conductance of the open-blocked state relative to the open state:

$$C' = C_{UT}C_{PT} + (1-g)O_{PT}$$

$$= C_U A_m \left(\frac{L_U + A}{A}\right)^m \left(1 + \left(\frac{\alpha_U \beta_P k_1 P}{\beta_U \alpha_P k_-}\right)\left(\frac{L_P + A}{L_U + A}\right)^m\right)$$

$$+ (1-g)\frac{\alpha_U k_1 P}{\beta_U k_-}\left(\frac{T_U}{T_P}\frac{(T_P + A)}{T_U + A)}\right)^n \quad \text{(A1)}$$

$$O' = O_T + gO_{TP} = O_U A_m \left(\frac{T_U + A}{T_U}\right)^n \left(1 + g\left(\frac{k_1 P}{k_-}\right)\left(\frac{T_U(T_P + A)}{T_P(T_U + A)}\right)^n\right). \quad \text{(A2)}$$

Hence,

$$\frac{C'}{O'} = \frac{\beta_U}{\alpha_U}\left(\frac{L_U + A}{A}\right)^n \left(\frac{T_U}{T_U + A}\right)^n$$

$$\cdot \left\{\frac{1 + \frac{\alpha_U}{\beta_U}\frac{\beta_P}{\alpha_P}\frac{k_1 P}{k_-}\left(\frac{L_P + A}{L_U + A}\right)^m + (1-g)\frac{\alpha_U k_1 P}{\beta_U k_-}\left(\frac{T_U}{T_P}\frac{(T_P + A)}{(T_U + A)}\right)^n}{1 + g\frac{k_1 P}{k_-}\left(\frac{T_U}{T_P}\frac{(T_P + A)}{(T_U + A)}\right)^n}\right\}. \quad \text{(A3a)}$$

If the activation curve is determined using an outward tail current measured at a potential where g approaches 1 at the peak of the tail current, then under those conditions,

$$\frac{C'}{O'} = \frac{\beta_U}{\alpha_U}\left(\frac{L_U + A}{A}\right)^n \left(\frac{T_U}{T_U + A}\right)^n \left\{\frac{1 + \frac{\alpha_U}{\beta_U}\frac{\beta_P}{\alpha_P}\frac{k_1 P}{k_-}\left(\frac{L_P + A}{L_U + A}\right)^m}{1 + \frac{k_1 P}{k_-}\left(\frac{T_U}{T_P}\frac{(T_P + A)}{(T_U + A)}\right)^n}\right\}. \quad \text{(A3b)}$$

At potentials around $V_{1/2}$ where g is negligible,

$$\frac{C'}{O'} = \frac{\beta_U}{\alpha_U}\left(\frac{L_U + A}{A}\right)^n \left(\frac{T_U}{T_U + A}\right)^n \left\{1 + \frac{\alpha_U}{\beta_U}\frac{\beta_P}{\alpha_P}\frac{k_1 P}{k_-}\left(\frac{L_P + A}{L_U + A}\right)^m + \frac{\alpha_U k_1 P}{\beta_U k_-}\left(\frac{T_U}{T_P}\frac{(T_P + A)}{(T_U + A)}\right)^n\right\}. \quad \text{(A3c)}$$

It is apparent from Eq. A3b that when the steady state voltage-activation curve is determined using outward tail currents where g approaches 1 then, when $k_1 P \ll k_-$

$$\frac{C'}{O'} = \frac{\beta_U}{\alpha_U}\left(\frac{L_U + A}{A}\right)^n \left(\frac{T_U}{T_U + A}\right)^n \quad \text{(A3d)}$$

and when $k_1 P \gg k_-$,

$$\frac{C'}{O'} = \frac{\beta_P}{\alpha_P}\left(\frac{L_P + A}{A}\right)^m \left(\frac{T_P}{A + T_P}\right)^n. \quad \text{(A3e)}$$

Kinetic Predictions

$$\alpha' C' = \alpha_U C_U A_m + \alpha_P C_P A_m$$

$$\alpha' = \frac{\alpha_U C_U A_m}{C_T + C_{TP}} + \frac{\alpha_P C_P A_m}{C_T + C_{TP}}$$

$$= \frac{\alpha_U C_U A_m}{C_T + C_{TP}} \left(1 + \frac{\beta_P}{\beta_U} \frac{k_1 P}{k_-}\right)$$

$$= \frac{\alpha_U \left(\frac{A}{L_U + A}\right)^m \left(1 + \frac{\beta_P}{\beta_U} \frac{k_1 P}{k_-}\right)}{1 + \frac{\alpha_U}{\beta_U} \frac{\beta_P}{\alpha_P} \frac{k_1 P}{k_-} \left(\frac{L_P + A}{L_U + A}\right)^m}. \quad \text{(A4a)}$$

Similarly,

$$\beta' C' = \beta_U O_U A_m + \beta_P O_P A_m$$

and,

$$\beta' = \frac{\beta_U \left(\frac{T_U}{T_U + A}\right)^n \left(1 + \frac{\beta_P}{\beta_U} \frac{K_1 P}{k_-}\right)}{1 + \frac{k_1 P}{k_-} \left(\frac{T_U}{T_P} \frac{(T_P + A)}{(T_U + A)}\right)^n}. \quad \text{(A4b)}$$

Comparing Eqs. A3b, and A4a,b it is apparent that as expected for a kinetic system with two predominant states,

$$\frac{C'}{O'} = \frac{\beta'}{\alpha'}.$$

Eqs. A4a,b also imply that when $k_1 P \ll k_-$ (e.g., when $F = 0$),

$$\alpha' = \alpha'_U = \alpha_U \left(\frac{A}{L_U + A}\right)^m; \qquad \beta' = \beta'_U = \beta_U \left(\frac{T_U}{T_U + A}\right)^n. \quad \text{(A4c,d)}$$

When $k_1 P \gg k_-$ (e.g., when $F = 1$)

$$\alpha' = \alpha'_P = \alpha_P \left(\frac{A}{L_P + A}\right)^m; \qquad \beta' = \beta'_P = \beta_P \left(\frac{T_P}{T_P + A}\right)^n. \quad \text{(A4e,f)}$$

Combining Eqs. A4c and A4e with equation A4b one obtains,

$$\alpha' = \frac{\alpha'_U \left(\frac{\beta_P}{\beta_U} \frac{k_1 P}{k_-}\right)}{1 + \frac{\beta_P}{\beta_U} \frac{k_1 P}{k_-} \frac{\alpha'_U}{\alpha'_P}}. \quad \text{(A5a)}$$

Similarly,

$$\beta' = \frac{\beta'_U\left(1 + \frac{\beta_P}{\beta_U}\frac{k_1 P}{k_-}\right)}{1 + \frac{\beta_P}{\beta_U}\frac{k_1 P}{k_-}\frac{\beta'_U}{\beta'_P}}. \tag{A5b}$$

Since at $V_{1/2}$, $\beta'_{1/2} = \alpha'_{1/2}$,

$$\frac{\beta'_{U,1/2}\left(1 + \frac{\beta_P}{\beta_U}\frac{k_1 P}{k_-}\right)}{1 + \frac{k_1 P}{k_-}\left(\frac{T_U}{T_P}\frac{(T_P + A)}{(T_U + A)}\right)^n}. \tag{A6}$$

Rearranging Eq. A6 and assuming that over the range of shift of $V_{1/2}$ with changing F (i.e., from -8 to -16 mV) that k_1P/k_-, β'_U and α'_U are relatively constant and that $(\beta_P/\beta_U)(k_1P/k_-) \ll 1$, one obtains,

$$\frac{k_1 P}{k_-} = \frac{\alpha'_{P,1/2}}{\alpha'_{U,1/2}}\frac{\beta_U}{\beta_P}\frac{(\alpha'_{U,1/2} - \alpha'_{1/2})}{(\alpha'_{1/2} - \alpha'_{P,1/2})} = \frac{\beta'_{P,1/2}}{\beta'_{U,1/2}}\frac{\beta_U}{\beta_P}\frac{(\beta'_{U,1/2} - \beta'_{1/2})}{(\beta'_{1/2} - \beta'_{P,1/2})}. \tag{A7}$$

Thus the change in rate constant with increasing F will be half maximal when,

$$\frac{k_1 P}{k_-} = \frac{\alpha'_{P,1/2}}{\alpha'_{U,1/2}}\frac{\beta_U}{\beta_P} = \frac{\beta'_{P,1/2}}{\beta'_{U,1/2}}\frac{\beta_U}{\beta_P} = \left(\frac{T_P\,(T_U + A)}{T_U\,(T_P + A)}\right)^n.$$

Voltage and Concentration Dependence of α' and β'

Pennefather et al. (1992) pointed out that in order for the line defining the relation between $\ln(\alpha')$ or $\ln(\beta')$ and voltage to shift in parallel with $\ln(A)$ the following equality must hold,

$$\frac{d\ln(\alpha')}{d\ln(A)} = \frac{d\ln(\alpha')}{B\,\mathrm{dV}}. \tag{A8}$$

If we differentiate Eq. A4c with respect to $\ln(A)$ we obtain,

$$\begin{aligned}\frac{d\ln(\alpha')}{d\ln(A)} = A\frac{d\ln(\alpha')}{dA} &= -mA\left(\frac{d\ln A}{dA} - \frac{d\ln(L + A)}{\mathrm{dA}}\right)\\ &= -mA\left(\frac{1}{A} - \frac{1}{L + A}\right)\\ &= -m\left(\frac{L}{L + A}\right).\end{aligned} \tag{A9}$$

If we differentiate Eq. A4c with respect to voltage we obtain

$$\frac{d\ln(\alpha'_U)}{dV} = \frac{d\ln(\alpha_U)}{dV} + m\frac{d\ln(A)}{dV} - m\frac{d\ln(L_U + A)}{dV} \tag{A10a}$$

$$= -xB - m\left(\frac{L_U}{L_U + A}\right)\frac{d\ln(L_U)}{dV}$$

$$= -xB - mzB\left(\frac{1}{1 + (A/L_{U,0})\exp[-zBV]}\right). \tag{A10b}$$

By combining Eqs. 8–10, one obtains a relation that defines the allowable values of x and z, required for the shift of $V_{1/2}$ as $[K^+]_o$ changes to parallel that of V_{rev}.

$$x = \frac{m(1 - z)}{1 + (A/L_{U,0})\exp[-zBV]}. \tag{A11}$$

Eq. A10a can be modified to consider how $\alpha'_{1/2}$ changes with $V_{1/2}$. For simplicity, we will consider the situation where $z = 0$.

$$\frac{d\ln(\alpha'_{U,1/2})}{dV_{1/2}} = \frac{d\ln(\alpha_{U,1/2})}{dV_{1/2}} + m\frac{d\ln(A)}{dV_{1/2}} - m\frac{d\ln(L_U + A)}{dV_{1/2}}$$

$$= -xB + m\frac{d\ln A}{dV_{1/2}}\left(1 - \frac{A}{L_U + A}\right)$$

$$= -xB + m\left(\frac{L_U}{L_U + A}\right)B\frac{dV_{rev,A}}{dV_{1/2}}.$$

Because

$$\frac{dV_{rev,A}}{dV_{1/2}} = 1 \text{ and accepting Eq. A11,}$$

$$\frac{d\ln(\alpha'_{U,1/2})}{dV_{1/2}} = -x + m\left(\frac{L_U}{L_U + A}\right) = 0. \tag{A12}$$

We thank Dr Peter Bachx for helpful comments on the manuscript.

This work was supported by Medical Research Council of Canada (Peter S. Pennefather) and by research grant HL 37500 and by Research Career Development Award K04-1928 (Thomas E. DeCoursey).

Original version received 13 August 1993 and accepted version received 22 December 1993.

REFERENCES

Adams, D. J., W. Nonner, T. M. Dwyer, and B. Hille. 1981. Block of endplate channels by permeant cations in frog skeletal muscle. *Journal of General Physiology.* 78:593–614.

Almers, W. 1971. The potassium permeability of frog muscle membrane. PhD dissertation. University of Rochester, Rochester, NY. 212 pp.

Armstrong, C. M. 1969. Inactivation of the potassium conductance and related phenomena caused by quaternary ammonium ion injection in squid axons. *Journal of General Physiology.* 54:553–575.

Armstrong, C. M. 1971. Interaction of tetraethylamonium ion derivatives with the potassium channel of giant axons. *Journal of General Physiology.* 58:413–437.

Ascher, P., A. Marty, and T. O. Neild. 1978. Life time and elementary conductance of the channels mediating the excitatory effects of acetylcholine in Aplysia neurones. *Journal of Physiology.* 278:177–206.

Benneton, P., and P. Christophersen. 1990. The gating of human red cell Ca^{2+} activated K^+ channels is strongly affected by the permeant cation species. *Biochimica et Biophysica Acta.* 1030:183–187.

Berry, R. M., and D. T. Edwards. 1993. Correlated ion flux through parallel pores: application to channel subconductance states. *Journal of Molecular Biology.* 133:77–84.

Burton, F. L., and O. F. Hutter. 1990. Sensitivity to flow of intrinsic gating in inwardly rectifying potassium channel from mammalian skeletal muscle. *Journal of Physiology.* 424:253–261.

Carmeliet, E. 1992. Extracellular Cs^+ ions block but also activate K^+ current in cardiac myocytes. *Biophysical Journal.* 61:251a. (Abst.)

Ciani, S., S. Krasne, S. Miyazaki, and S. Hagiwara. 1978. A model for anomalous rectification: electrochemical-potential-dependent gating of membrane channels. *Journal of Membrane Biology.* 44:103–134.

Cohen, I. S., D. DiFrancesco, N. K. Mulrine, and P. Pennefather. 1989. Internal and external K^+ help gate the inward rectifier. *Biophysiology Journal.* 55:197–202.

Demo, S. D., and G. Yellen. 1992. Ion-effects on gating of the Ca^{2+} activated K^+ channel correlate with occupancy of the pore. *Biophysical Journal.* 61:639–648.

Draber, S., R. Schultze, and U.-P. Hansen. 1991. Patch-clamp studies on the anomalous mole fraction effect of the K^+ channel in cytoplasmic droplets of Nitella. *Journal of Membrane Biology.* 123:183–190.

Ermishkin, L. N., Kh.M. Kasumov, and V. M. Potseluyev. 1977. Properties of amphotericin B channels in a lipid bilayer. *Biochimica et Biophysica Acta.* 470:357–367.

Hagiwara, S., S. Miyazaki, S. Krasne, and S. Ciani. 1977. Anomalous permeabilities of the egg cell membrane of a starfish in K^+-Tl^+. *Journal of General Physiology.* 70:269–281.

Hagiwara, S., and K. Takahashi. 1974. The anomalous rectification and cation selectivity of the membrane of a starfish egg cell. *Journal of Membrane Biology.* 18:61–80.

Hanke, W., and C. Miller. 1983. Single chloride channels from Torpedo electroplax: activation by protons. *Journal of General Physiology.* 82:25–45.

Hill, T. L., and Y-D. Chen. 1971. On the theory of ion-transport across the nerve membrane, II. Potassium ion kinetics and cooperativity (with x = 4). *Proceedings of the National Academy of Sciences, USA.* 68:1711–1715.

Hille, B., and W. Schwartz. 1978. Potassium channels as multi-ion single-file pores. *Journal of General Physiology.* 72:409–442.

Horowicz, P., P. W. Gage, and R. S. Eisenberg. 1968. The role of the electrochemical gradient in determining potassium fluxes in frog striated muscle. *Journal of General Physiology.* 51:193*s*–203*s*.

Hutter, O. F., and T. L. Williams. 1979. A dual effect of formaldehyde on the inwardly rectifying potassium conductance in skeletal muscle. *Journal of Physiology.* 286:591–606.

Ishihara, K., T. Mitsuiye, A. Noma, and M. Takano. 1989. The Mg^{2+} block and intrinsic gating underlying inward rectification of the K^+ current in guinea-pig cardiac myocytes. *Journal of Physiology.* 419:297–320.

Kirsch, G. E., J. E. Drewe, M. Taglialatella, R. H. Joho, M. DeBiasi, H. A. Hartmann, and A. M. Brown. 1992. A single nonpolar residue in the deep pore of related K^+ channels acts as a K^+:Rb^+ conductance switch. *Biophysical Journal.* 62:136–144.

Krouse, M. E., G. T. Schneider, and P. W. Gage. 1986. A large anion-selective channel has seven conductance levels. *Nature.* 319:58–60.

Kubo, Y., T. J. Baldwin, Y. N. Jan, and L. Y. Jan. 1993. Primary structure and functional expression of a mouse inwardly rectifying potassium channel. *Nature.* 362:127–133.

Kolb, H.-A., and E. Bamberg. 1977. Influence of membrane thickness and ion concentration on the properties of the gramicidin a channel: autocorrelation, spectral power density, relaxation and single-channels studies. *Biochimica et Biophysica Acta.* 464:127–141.

Lee, C.-Y. 1992. A possible biological role of the electron transfer between tyrosine and tryptophan: gating of ion channels. *FEBS Letters.* 299:119–123.

Leech, C. A., and P. R. Stanfield. 1981. Inward rectification in frog skeletal muscle fibres and its dependence on membrane potential and external potassium. *Journal of Physiology.* 319:295–309.

Liman E. R., P. Hess, F. Weaver, and G. Koren. 1991. Voltage sensing particle in the S-4 region of a mammalian K^+ channel. *Nature.* 353:752–756.

MacKinnon, R. 1991. Determination of the subunit structure of a voltage gated potassium channel. *Nature.* 350:232–235.

Matsuda, H., A. Saigusa, and H. Irisawa. 1987. Ohmic conductance through the inwardly rectifying K channel and blocking by interval Mg^{2+}. *Nature.* 325:156–159.

Matsuda, H. 1988. Open-state substructure of inwardly rectifying potassium channels revealed by magnesium block in guinea-pig heart cells. *Journal of Physiology.* 397:237–258.

Matsuda, H., H. Matsuura, and A. Noma. 1989. Triple barrel structure if inwardly rectifying K^+ channel revealed by Cs^+ and Rb^+ block in guinea pig heart cells. *Journal of Physiology.* 413:139–157.

Matsuda, H. 1991. Effects of external and internal K^+ ions on magnesium block of inwardly rectifying K^+ channels in guinea-pig heart cells. *Journal of Physiology.* 435:83–99.

Miller, C. R., R. Latorre, and I. Reisin. 1987. Coupling of voltage-dependent gating and Ba^{++} block in the high-conductance Ca^{++} activated K^+ channel. *Journal of General Physiology.* 90:427–449.

Mitra, R. L., and M. Morad. 1991. Permeance of Ca^{++} and Rb^+ through the inwardly rectifying K^+ channel in guinea pig ventricular myocytes. *Journal of Membrane Biology.* 122:33–42.

Neher, E., and J. H. Steinbach. 1978. Local anesthetics transiently block currents through single acetylcholine receptor channels. *Journal of Physiology.* 277:153–176.

Neyton, J., and M. Pelleschi. 1991. Multi-ion occupancy alters gating in high-conductance, Ca^{2+} activated K^+ channels. *Journal of General Physiology.* 97:549–567.

Neyton, J., and C. Miller. 1988. Potassium blocks barium permeation through a calcium-activated potassium channel. *Journal of General Physiology.* 92:549–567.

Nilius, B., and D. Riemann. 1990. Ion channels in human endothelial cells. *General Physiology and Biophysics.* 9:89–112.

Oliva, C., I. S. Cohen, and P. Pennefather. 1990. The mechanism of rectification of i_{K1} in canine Purkinje myocytes. *Journal of General Physiology.* 96:299–318.

Pennefather, P., and D. M. J. Quastel. 1980. Actions of anesthetics on the function of nicotinic acetylcholine receptors. *In* Progress in Anesthesiology. Vol 2. Molecular Mechanisms of Anesthetics. B. R. Fink, editor. Raven Press, New York. 157–168.

Pennefather, P., C. Oliva, and N. Mulrine. 1992. Origin of the potassium and voltage dependence of the cardiac inwardly rectifying K-current (I_{K1}). *Biophysical Journal.* 61:448–462.

Pardo, L. A., S. H. Heinemann, H. Terlau, U. Ludewig, C. Lorra, O. Pongs, and W. Stuhmer. 1992. Extracellular K^+ specifically modulates a rat brain K^+ channel. *Proceedings of the National Academy of Sciences, USA.* 89:2466–2470.

Shapiro, M. S., and T. E. DeCoursey. 1991. Permeant ion effects on the gating kinetics of the type L potassium channel in mouse lymphocytes. *Journal of General Physiology.* 97:1251–1278.

Shioya, T., A. Matsuda, and A. Noma. 1993. Fast and slow blockade of the inward rectifier K^+ channel by external divalent cations in guinea pig myocytes. *Pflügers Archiv.* 422:427–435.

Silver, M. R., and T. E. DeCoursey. 1990. Intrinsic gating of inward rectifier in bovine pulmonary artery endothelial cells in the presence or absence of internal Mg^{2+}. *Journal of General Physiology.* 96:109–133.

Silver, M. R., M. S. Shapiro, and T. E. DeCoursey. 1994. Effects of external Rb^+ on inward rectifier K^+ channels of bovine pulmonary artery endothelial cells. *Journal of General Physiology.* 103:519–548.

Standen, N. B., and P. R. Stanfield. 1980. Rubidium block and rubidium permeability of the inward rectifier of frog skeletal muscle. *Journal of Physiology.* 304:415–435.

Stanfield, P. R., F. M. Ashcroft, and T. D. Plant. 1981. Gating of a muscle K^+ channel and its dependence on the permeating ion species. *Nature.* 289:509–511.

Tourneur, Y., R. Mitra, M. Morad, and O. Rougier. 1987. Activation properties of the inward-rectifying potassium channel of mammalian heart cells. *Journal of Membrane Biology.* 97:127–135.

Van Helden, D., O. P. Hamill, and P. W. Gage. 1977. Permeant cations alter channel characteristics. *Nature.* 269:711–713.

Vandenberg, C. A. 1987. Inward rectification of a potassium channel in cardiac ventricular cells depends on internal magnesium ions. *Proceedings of the National Academy of Sciences, USA.* 84:2560–2564.

Woodhull, A. M. 1973. Ionic blockage of sodium channels in nerve. *Journal of General Physiology.* 61:687–708.

Yang, X.-C., and F. Sachs. 1990. Characterization of stretch-activated ion channels in *Xenopus* oocytes. *Journal of Physiology.* 431:103–122.